National Library
of Canada

Acquisitions and
Bibliographic Services Branch

395 Wellington Street
Ottawa, Ontario
K1A 0N4

Bibliothèque nationale
du Canada

Direction des acquisitions et
des services bibliographiques

395, rue Wellington
Ottawa (Ontario)
K1A 0N4

Your file Votre référence

Our file Notre référence

NOTICE

The quality of this microform is heavily dependent upon the quality of the original thesis submitted for microfilming. Every effort has been made to ensure the highest quality of reproduction possible.

If pages are missing, contact the university which granted the degree.

Some pages may have indistinct print especially if the original pages were typed with a poor typewriter ribbon or if the university sent us an inferior photocopy.

Reproduction in full or in part of this microform is governed by the Canadian Copyright Act, R.S.C. 1970, c. C-30, and subsequent amendments.

AVIS

La qualité de cette microforme dépend grandement de la qualité de la thèse soumise au microfilmage. Nous avons tout fait pour assurer une qualité supérieure de reproduction.

S'il manque des pages, veuillez communiquer avec l'université qui a conféré le grade.

La qualité d'impression de certaines pages peut laisser à désirer, surtout si les pages originales ont été dactylographiées à l'aide d'un ruban usé ou si l'université nous a fait parvenir une photocopie de qualité inférieure.

La reproduction, même partielle, de cette microforme est soumise à la Loi canadienne sur le droit d'auteur, SRC 1970, c. C-30, et ses amendements subséquents.

Canada

UNIVERSITY OF ALBERTA

FORMULATION OF SUSTAINED RELEASE MICROPARTICLES OF A BACTERIAL NUTRIENT AND AN ANTIHISTAMINE

BY

IO SAN (ELKA) LAO

©

A THESIS

SUBMITTED TO THE FACULTY OF GRADUATE STUDIES AND RESEARCH IN
PARTIAL FULFILLMENT OF THE REQUIREMENT FOR THE DEGREE OF

MASTER OF SCIENCE

IN

PHARMACEUTICAL SCIENCES (PHARMACEUTICS)

Faculty of Pharmacy and Pharmaceutical Sciences

EDMONTON, ALBERTA

Spring, 1993

National Library
of Canada

Acquisitions and
Bibliographic Services Branch

395 Wellington Street
Ottawa, Ontario
K1A 0N4

Bibliothèque nationale
du Canada

Direction des acquisitions et
des services bibliographiques

395, rue Wellington
Ottawa (Ontario)
K1A 0N4

Your file Votre référence

Our file Notre référence

The author has granted an irrevocable non-exclusive licence allowing the National Library of Canada to reproduce, loan, distribute or sell copies of his/her thesis by any means and in any form or format, making this thesis available to interested persons.

L'auteur a accordé une licence irrévocable et non exclusive permettant à la Bibliothèque nationale du Canada de reproduire, prêter, distribuer ou vendre des copies de sa thèse de quelque manière et sous quelque forme que ce soit pour mettre des exemplaires de cette thèse à la disposition des personnes intéressées.

The author retains ownership of the copyright in his/her thesis. Neither the thesis nor substantial extracts from it may be printed or otherwise reproduced without his/her permission.

L'auteur conserve la propriété du droit d'auteur qui protège sa thèse. Ni la thèse ni des extraits substantiels de celle-ci ne doivent être imprimés ou autrement reproduits sans son autorisation.

ISBN 0-315-82219-8

Canadä

UNIVERSITY OF ALBERTA

RELEASE FORM

NAME OF AUTHOR: **IO SAN (ELKA) LAO**

TITLE OF THESIS: **FORMULATION OF SUSTAINED RELEASE MICROPARTICLES OF A BACTERIAL NUTRIENT AND AN ANTIHISTAMINE**

DEGREE: **MASTER OF SCIENCE**

YEAR THIS DEGREE GRANTED: SPRING, 1993

Permission is hereby granted to the **University of Alberta** Library to reproduce single copies of this thesis and to lend or sell such copies for private, scholarly or scientific research purposes only.

The author reserves all other publication and other rights in association with the copyright in the thesis, and except as hereinbefore provided neither the thesis nor any substantial portion thereof may be printed or otherwise reproduced in any material from whatever without the author's prior written permission.

LAO IO SAN.

Permanent address:
No. 111 Ave Ouv Arriaga
2º Andar (A). Macau

Date: Feb. 17, 1993

UNIVERSITY OF ALBERTA

FACULTY OF GRADUATE STUDIES AND RESEARCH

The undersigned certify that they have read, and recommend to the Faculty of Graduate Studies and Research for acceptance, a thesis entitled **Formulation of sustained release microparticles of a bacterial nutrient and an antihistamine** submitted by **Io San (Elka) Lao** in partial fulfillment of the requirements for the degree of **Master of Science**.

J. A. Rogers
Dr. J. A. Rogers

Dr. L. I. Wiebe

B. Kratochvil
Dr. B. Kratochvil

Date : Feb. 12, 1993

Dedicated

To

MY PARENTS AND GRANDMOTHER

ABSTRACT

Methyl methacrylate (MMA) and its polymer (PMMA) were used to prepare PMMA microcapsules of Brain Heart Infusion Medium by employing in-situ polymerization and spray drying techniques, respectively. The microcapsules formed were spherical and had a mean size less than 5 μm in diameter. The release of BHIM was fairly rapid which was likely due to defects in the microcapsules wall as seen by SEM. In contrast, poly(L-lysine terephthaloyl chloride) (PLT) and poly(piperazine terephthaloyl chloride) (PPT) microcapsules of BHIM prepared by an interfacial polymerization method, were less than 4 μm, had a loading of BHIM from 20 to 50 percent, and sustained release of BHIM for up to 40 days.

Sustained release ethylcellulose microspheres of dimenhydrinate, an antihistamine having a water solubility of about 1 percent, were prepared by the solvent evaporation process. The microspheres accommodated a drug loading varying from 20 to 96 percent, and exhibited free-flowing properties. The method was shown to be reproducible with respect to both drug loading and microsphere size distribution. The release of dimenhydrinate in water at 37°C was observed for 5 hr and obeyed either first-order or $t^{1/2}$ kinetics (Higuchi model) depending on the polymer-drug ratio and preparation conditions, compared to the complete dissolution of an equivalent amount of drug within 30 min. The microspheres observed by SEM had a sponge-like appearance made up of compressed strands of polymer in which drug was dispersed suggesting that release occurred by a

dissolution-diffusion mechanism.

Microcapsules of diphenhydramine HCl (solubility is approx. 1g/ml) prepared with Eudragit RS 100 by a coacervation technique were irregularly-shaped. Although the release profiles were slightly altered by the polymer concentration used or the amount of polyisobutylene included as an anti-aggregating agent, they were not significantly different than the dissolution profile of diphenhydramine HCl.

ACKNOWLEDGEMENTS

I wish to express my gratefulness and thanks to Dr. J. A. Rogers for his excellent supervision, guidance, and valuable advice rendered during the course of the program. His motivation, enthusiasm, and patience helped me a great deal in achieving the research goals.

I sincerely thank the members of my committee for their valuable suggestions. I thank the Faculty of pharmacy and pharmaceutical sciences for providing financial assistance. The help of fellow graduate students throughout the program was deeply appreciated.

Finally, I would like to thank the members of my family for their loving support.

Table of Contents

CHAPTER PAGE

1. INTRODUCTION 2

2. BACKGROUND 4
  2.1. Definition, Nomenclature and Classification 4
    2.1.1. Definition 4
    2.1.2. Nomenclature 4
    2.1.3. Classification 5
  2.2. Materials and General Techniques 5
    2.2.1. Pan Coating 6
    2.2.2. Spray Drying 6
    2.2.3. Air Suspension Coating 6
    2.2.4. Coacervation-Phase Separation Procedures 7
    2.2.5. Solvent Evaporation 8
    2.2.6. Suspension Crosslinking 8
    2.2.7. Suspension Polymerization 8
    2.2.8. Emulsion Polymerization 9
    2.2.9. In-situ Polymerization 9
    2.2.10. Interfacial Polymerization 10
  2.3. Types of Core Materials 10
  2.4. Design of Controlled Release Microparticles 11
    2.4.1. Diffusion Controlled Systems 12
      2.4.1.1. The reservoir system 12
      2.4.1.2. The matrix system 13
    2.4.2. Chemically Controlled Systems 14
      2.4.2.1. Bioerodible system 14
      2.4.2.2. Pendent chain system 16
    2.4.3. Swelling Controlled System 17

2.5. Kinetics of Agent Release 18
    2.5.1. Zero-order Release Kinetics 20
    2.5.2. First-order Release Kinetics 21
    2.5.3. Matrix Release Kinetics. The Higuchi Model 22
2.6. General Safety Considerations 25
    2.6.1. Environment Concern 25
    2.6.2. Public Health Concern 26
2.7. Industrial Applications 27
    2.7.1. Agricultural 27
    2.7.2. Pharmaceutical 30
    2.7.3. Enhanced Oil Recovery Processes 31

3. AIMS AND SCOPE OF THE THESIS 36
3.1. Microencapsulation of A Nutrient (BHIM) 36
    3.1.1. Aim 36
    3.1.2. Objectives of SR Microcapsules of BHIM 37
3.2. Microencapsulation of Antihistamine Drugs 38
    3.2.1. Aim 38
    3.2.2. Objectives of SR Microparticle Formulation of Antihistamines 39

4. EXPERIMENTAL 41
4.1. Microencapsulation of Brain Heart Infusion Medium 41
    4.1.1. Preparation of PMMA Microcapsules by Spray Drying Technique 41
        4.1.1.1. Materials 41
        4.1.1.2. Preparation of spray-dried BHIM powder 41
        4.1.1.3. Preparation of BHIM-loaded PMMA microcapsules 41
        4.1.1.4. Microscopic studies 42
        4.1.1.5. Release studies 42

4.1.2. Preparation of PMMA Microcapsules by In-situ Polymerization 43
    4.1.2.1. Materials 43
    4.1.2.2. Preparation of PMMA microcapsules 43
    4.1.2.3. SEM studies 44
4.1.3. Preparation of Polyamide Microcapsules by Interfacial Polymerization 44
    4.1.3.1. Materials 44
    4.1.3.2. Preparation of BHIM solution 44
    4.1.3.3. Preparation of polyamide microcapsules 45
    4.1.3.4. SEM studies 47
    4.1.3.5. Characterization of PLT and PPT microcapsules 47
    4.1.3.6. Release studies of polyamide microcapsules . . . 47
4.2. MICROENCAPSULATION OF DIMENHYDRINATE 48
4.2.1. Materials 48
4.2.2. Preparation of Microparticles 48
4.2.3. Microscopic Studies 49
4.2.4. Size Analysis of Microparticles 49
4.2.5. Determination of Dimenhydrinate Loading 49
4.2.6. Release Studies 49
4.3. MICROENCAPSULATION OF DIPHENHYDRAMINE HCL . . 50
4.3.1. Ethylcellulose Microcapsules 50
    4.3.1.1. Materials 50
    4.3.1.2. Method of preparation. 50
    4.2.1.3. Optical microscopic studies 51
    4.2.1.4. Diphenhydramine HCl content 51
    4.2.1.5. Release studies 51
4.3.2. Eudragit RS 100 Microcapsules 52
    4.3.2.1. Method of preparation 52
    4.3.2.2. Microscopic studies 52
    4.3.2.3. Diphenhydramine HCl content 53
    4.3.2.4. Release studies 53

5. RESULTS 55
5.1. MICROENCAPSULATION OF BHIM 55
5.1.1. PMMA Microcapsules by Spray Drying 55
5.1.1.1. Size and shape analysis by SEM 55
5.1.1.2. *In vitro* release 55
5.1.2. PMMA Microcapsules by In-situ Polymerization 55
5.1.2.1. Size and shape analysis by SEM 55
5.1.3. Polyamide Microcapsules by Interfacial Polymerization 58
5.1.3.1. Size and shape analysis by SEM 58
5.1.3.2. BHIM loading, encapsulation efficiency and yield of microcapsules 58
5.1.3.3. *In vitro* release 59
5.2. MICROENCAPSULATION OF DIMENHYDRINATE 72
5.2.1. Process Evaluation of the Technique 72
5.2.1.1. Effect of stirring rate 72
5.2.1.2. Influence of surfactant 77
5.2.2. Test of Reproducibility of the Method 77
5.2.2.1. Particle size distribution 77
5.2.2.2. Drug content of microspheres 78
5.2.3. Microspheres at Various Polymer:Drug Ratios 84
5.2.3.1. Particle size distribution 84
5.2.3.2. Efficiency of drug loading 84
5.2.4. Drug Release Studies 88
5.3. MICROENCAPSULATION OF DIPHENHYDRAMINE HCL . . 91
5.3.1. Examination of Microcapsules by OM and SEM 94
5.3.2. Effect of Eudragit RS 100 Concentrations on *In Vitro* Release 94
5.3.3. Effect of PIB Concentrations. 95

6. DISCUSSION 101
6.1. BHIM 101
6.2. Dimenhydrinate 105

6.3. Diphenhydramine HCl 112

7. CONCLUSIONS 115

REFERENCES. 117

APPENDIX. 125

LIST OF TABLES

Table 2.1 General microencapsulation techniques 5

Table 2.2 Microencapsulation techniques available for water-soluble and water-insoluble materials 11

Table 5.1 Loading of BHIM in polyamide microcapsules prepared at two BHIM concentrations 60

Table 5.2 Yield of polyamide microcapsules prepared at two BHIM concentrations 61

Table 5.3 Encapsulation efficiency of BHIM in polyamide microcapsules prepared at two BHIM concentrations 63

Table 5.4 Statistical analysis (t-test) of polyamide microcapsule formulation parameters of two BHIM concentrations (20% and 40% w/v) 64

Table 5.5 Comparison of release rate constant (k) of BHIM from polyamide microcapsules at two concentrations of BHIM solution at 23°C 68

Table 5.6 Comparison of release rate constant (k) of BHIM from polyamide microcapsules prepared with 20% w/v BHIM solution at two temperatures 71

Table 5.7 Size analysis of ethylcellulose microspheres of dimenhydrinate (1:3 polymer:drug) 74

Table 5.8 Size analysis of different batches of ethylcellulose microspheres of dimenhydrinate (1:3 polymer:drug) prepared at 300 rpm 79

Table 5.9 Dimenhydrinate content of ethylcellulose 20/40 sieve size microspheres (1:3 polymer:drug) prepared at 300 rpm 82

Table 5.10 Analysis of variance of results in Table 5.9 83

Table 5.11 Comparison of the drug contents of two sieve size fractions of dimenhydrinate ethylcellulose microspheres formulations with different drug loadings 87

Table 5.12 Comparison of the T_{50} of dimenhydrinate from ethylcellulose microspheres of sieve size fraction 20/40 and 40/60 prepared at three drug loadings 92

Table 6.1 First-order release rate constant of dimenhydrinate from ethylcellulose microspheres of sieve size 20/40 and 40/60 prepared under different conditions 111

LIST OF FIGURES

Figure 2.1 Some typical structures of microcapsules 4

Figure 2.2 Diagram showing the cross-section of a spherical diffusion-controlled membrane-enclosed reservoir system 12

Figure 2.3 Diagram showing the cross-section of a spherical diffusion-controlled matrix system with dispersed agent 14

Figure 2.4 Diagram showing the cross-section of a spherical bioerodible sphere 15

Figure 2.5 Schematic diagram of three mechanisms of bioerosion 16

Figure 2.6 Diagram of a chemically-controlled pendent chain delivery system 17

Figure 2.7 Diagram of the cross-section of a spherical swelling-controlled matrix 18

Figure 2.8 Concentration gradient across an ideal isotropic polymeric membrane (K<1) 20

Figure 2.9 Diagram of agent distribution and concentration gradients within an idealized rectangular or slab matrix (monolith) as a function of time 24

Figure 2.10 Relationship between the level of application and the duration of action of conventional and controlled release formulations 28

Figure 4.1 Schematic diagram of the apparatus for electrocapillary emulsification 45

Figure 5.1 Scanning electron micrographs of BHIM powder and PMMA microcapsules 56

Figure 5.2 Scanning electron micrograph of PMMA microcapsules prepared from 1% w/v potassium persulfate and 11.8% v/v MMA at 80°C 57

Figure 5.3 Scanning electron micrograph of PPT microcapsules suspended in 50% Tween 20 solution 59

Figure 5.4 The effect of BHIM concentration on the release of protein from PLT microcapsules at 23°C 65

Figure 5.5 The effect of BHIM concentration on the release of protein from PPT microcapsules at 23°C 66

Figure 5.6 The effect of temperature on the release of protein from PLT microcapsules prepared with 20% w/v BHIM solution 69

Figure 5.7 The effect of temperature on the release of protein from PPT microcapsules prepared with 20% w/v BHIM solution 70

Figure 5.8 Scanning electron micrographs of ethylcellulose microspheres of dimenhydrinate sieve size fraction 20/40 1:3 polymer:drug prepared at 300 rpm 73

Figure 5.9 Size distribution of ethylcellulose microspheres of dimenhydrinate (1:3 polymer:drug) prepared at two stirring rates 75

Figure 5.10 Log-probability plots for size distribution of ethylcellulose microspheres of dimenhydrinate (1:3 polymer:drug) prepared at two stirring rates 76

Figure 5.11 Size distribution of three batches of ethylcellulose microspheres of dimenhydrinate prepared at 300 rpm 80

Figure 5.12 Log-probability plots of the size distribution of three batches of ethylcellulose microspheres prepared at 300 rpm 81

Figure 5.13 Size distribution of ethylcellulose microspheres of dimenhydrinate prepared at different stirring rates 85

Figure 5.14 Log-probability plots of the size distribution of ethylcellulose microspheres at various drug loadings prepared at two stirring rates 86

Figure 5.15 Release of dimenhydrinate from two different sieve size ranges of ethylcellulose microspheres prepared at 300 rpm in water at 37°C 89

Figure 5.16 Release of dimenhydrinate from two different sieve size ranges of ethylcellulose microspheres prepared at 400 rpm in water at 37°C 90

Figure 5.17 Dependence of the time for 50 percent dimenhydrinate release (T_{50}) from ethylcellulose microspheres 425-841 µm prepared at 400 rpm as a function of weight percentage of coating material 93

Figure 5.18 Optical micrograph of 8% w/v Eudragit RS 100 microcapsules of diphenhydramine HCl 96

Figure 5.19 Scanning electron micrograph of 8% w/v Eudragit RS 100 microcapsule of diphenhydramine HCl 97

Figure 5.20 Release of diphenhydramine HCl in pH 7.4 phosphate buffer at 37°C from 40/60 sieve size microcapsules as a function of Eudragit RS 100 concentration 98

Figure 5.21 Release of diphenhydramine HCl from 8% w/v Eudragit RS 100 microcapsules of sieve size 40/60 as a function of PIB concentration 99

Figure 6.1 First-order plots of dimenhydrinate remaining versus time of two sieve size ranges of microspheres prepared at 300 rpm 108

Figure 6.2 First-order plots of dimenhydrinate remaining versus time of two sieve size ranges of microspheres prepared at 400 rpm 109

Figure 6.3 Plot of percentage of dimenhydrinate released versus $t^{1/2}$ from 1:1 polymer:drug sieve size fraction 20/40 microspheres prepared at 400 rpm 110

LIST OF ABBREVIATIONS

A	Cross-sectional release area of a slab.
BHIM	Brain Heart Infusion Medium.
C	Molar concentration of solute A.
C_h	High concentration solution side.
C_l	Low concentration solution side.
C_m	Concentration of agent in the membrane.
C_{max}	Maximum plasma concentration.
C_{min}	Minimum plasma concentration.
$C_{m(h)}$	Membrane solute concentration in the high concentration side.
$C_{m(l)}$	Membrane solute concentration in the low concentration side.
C_s	Solubility of the agent in the matrix.
C_{sw}	Solubility of the agent in the permeating fluid.
C_{tot}	Total amount of agent present in the matrix per unit volume.
CNS	Central nervous system.
ΔC_m	Difference in agent concentration between solutions on either side of the membrane.
D	Agent diffusion coefficient in the membrane.
D_A	Binary diffusion coefficient or mass diffusivity.
D_w	Agent diffusion coefficient in the permeating fluid.
Darcy	Permeability, in the unit of cm^2.
EOR	Enhanced oil recovery.
J_A	Molar flux of solute A.
K	Partition coefficient between the polymer membrane and aqueous environment.
k'	First-order rate constant.
k_1	Proportional constant.
k_p	Propagation rate constant.

k_t	Overall termination constant.
M	Amount of agent released.
M_{it}	Mass of agent remaining at any time in the internal reservoir.
M_{tot}	Total agent in the system.
MEOR	Microbial enhanced oil recovery.
[M]	Monomer concentration.
mg	Milligram.
ml	Milliliter.
NLh^{-1}	Normliter per hour.
PIB	Polyisobutylene.
ϕ	Porosity of the leached portion of the matrix.
PLT	Poly(L-lysine terephthaloyl chloride).
PPT	Poly(piperazine terephthaloyl chloride).
Q	Amount of agent released after time t per unit exposed area.
r_o	Outside radii of the microcapsule.
r_i	Inside radii of the microcapsule.
S	Surface area of the membrane.
SEM	Scanning electron microscopy.
SR	Sustained release.
T_{50}	Time taken for 50% drug released.
t	Time.
τ	Tortuosity factor of the capillary system.
UMB	Ultramicrobacteria.
uv	Ultraviolet.
V_i	Volume of the internal reservoir.
X_m	Membrane thickness.
x_A	Molar fraction of solute A.

CHAPTER I

1. INTRODUCTION

The first research leading to the development of microencapsulation was published by Bungenburg de Jong and Kass on studies of coacervation in 1931[1]. Coacervation also appears to be the earliest microencapsulation technique, developed by the National Cash Register (NCR) Company in the 1950s to produce microencapsulated tiny droplets of crystal violet lactone solution, a dye precursor used in carbonless copy paper[2-4]. In this process, microcapsules were affixed to the under surface of a sheet of paper and dye was released upon rupture of the microcapsules due to the pressure from the tip of the writing instrument.

The advent of carbonless copy paper has, subsequently, led to extensive studies on microencapsulation. Within the past several decades, a variety of microencapsulation techniques have been developed in different fields to separate incompatible chemical entities, to convert liquid to free-flowing powder, to produce controlled-release profiles, to protect compounds from decomposition, and to mask foul odours or tastes[5-6]. Among these, sustained and controlled release formulation has yielded the greatest benefits and thus aroused considerable interest in a variety of industries[7-9].

Generally, microencapsulated product refers to microparticles varying in size from about 10 nm to 5 mm. Most agents which have been microencapsulated are lipophilic and only a few water-soluble agents have been successfully formulated[10]. Factors that are important to consider in microencapsulation include, type of polymer, method of preparation, characteristics of the material to be microencapsulated, in conjunction with the polymerization process, particle shape, the size of the materials to be encapsulated and the relative solubilities of polymer and materials in the solvents to be used.

The microencapsulation of water-soluble agents could have applicability in many areas but the two in particular which have been addressed in this thesis are: 1) the microencapsulation of enhanced oil recovery materials, and 2) the microencapsulation of water-soluble antihistamines for sustained oral administration. The specific objectives which were tested included 1) the microencapsulation of an energy-rich material, Brain Heart Infusion Medium (BHIM) in microbial enhanced oil recovery (MEOR), for co-injection with bacteria to improve conformance in waterflooding processes of oil extraction, and 2) the microencapsulation of two antihistamines, diphenhydramine hydrochloride which has a water-solubility of 1 g/ml, and dimenhydrinate which has a water-solubility of 1 g/95 ml. If sustained release of the antihistamines is achieved the main benefits are that the side-effects associated with these drugs and the dose frequency would be reduced.

2. BACKGROUND

2.1. Definition, Nomenclature and Classification

2.1.1. Definition

Microencapsulation can be defined as the incorporation of material in small polymer particles which have an arbitrary particle size ranging from approximately 10 nm to 5 mm. Within this broad definition, microparticles have included solid, liquid or gaseous substances[11].

2.1.2. Nomenclature

Depending on the manufacturing process, different structures of microencapsulated products are often obtained and because of this, there is considerable confusion in the nomenclature of the resulting microparticles[6,12]. In this thesis, the term microcapsule is defined as a microparticle having a thin polymeric coating surrounding a core material. Some typical structures of microcapsules are shown in Figure 2.1[10]. When no distinct coating and core regions are distinguishable, the microparticles are then referred to as microspheres.

Figure has been removed due to copyright.

Figure 2.1 Some typical structures of microcapsules (taken from P. B. Deasy, Ref. 10).

2.1.3. Classification

Classification of the known microencapsulation processes is very important for better understanding and optimum application of the technology. Classifications proposed by Sliwka[13], Kondo[6] and Thies[14] lack universality since they do not cover all of the known processes. The classification currently proposed by Arshby[15] is adopted in this thesis because of its versatility, in categorizing the types of starting materials used in the processes. Table 2.1 lists the general microencapsulation techniques.

Table 2.1. General microencapsulation techniques

From monomeric starting materials	From polymeric starting materials
suspension polymerization	pan coating
emulsion polymerization	spray drying
interfacial polymerization	fluidized bed coating/air suspension coating
in-situ polymerization	coacervation/phase separation
	solvent evaporation
	suspension crosslinking

2.2. Materials and General Techniques

A great many microencapsulation techniques are available and new ones are being developed each year. Microencapsulated products can be manufactured from a large number of starting materials and by as many different polymerization techniques[16-18] and microencapsulation processes[10]. The general microencapsulation techniques are briefly described below.

2.2.1. Pan Coating

This process, widely used in the pharmaceutical industry, is among the oldest procedures for coating tablets or even small particles or beads. The beads or tablets are tumbled in a pan or other similar device while coating material is slowly applied. A wide variety of organic solvent-based or water-based polymers may be employed using this technique[19]. The microparticle size range produced is usually in the range of 200 to 5000 μm.

2.2.2. Spray Drying

Spray drying consists of spraying an emulsion or a solution of polymer and agent in a stream of hot, inert gas. A number of control parameters must be considered in order to obtain the optimum conditions, including nozzle flow rate, aspirator setting, inlet/outlet temperatures, and other factors[20]. Its main advantage is the ability to handle heat labile materials because of the short contact time in the drying chamber. In addition, the resulting particles are obtained as a free-flowing, dry powder. Many water-soluble and water-insoluble materials can be microencapsulated by this process. The particle size obtained varies from about 8 to 800 μm.

2.2.3. Air Suspension Coating

This is the most widely used process in the pharmaceutical industry for the microencapsulation of drugs since it provides better control and flexibility in the properties of the final product. It is often referred to as the Wurster coating technique after Dale Wurster who filed several patents on a modified fluidized bed coater[21]. Finely-divided solid core material is suspended by a vertical current of air, then sprayed with a solution of coating material. As the solvent evaporates, a membrane of the coating material is deposited around each particle. A great variety of coating materials have been used including waxes, cellulosic compounds or water-soluble polymers using aqueous or organic vehicles, as appropriate. This technique lends itself to coating solid particles with diameters ranging from 50 μm up to tablet size.

2.2.4. Coacervation-Phase Separation Procedures

Coacervation was the first microencapsulation technique used and remains one of the most widely used[7]. Coacervation may occur either by gradual desolvation of polymer molecules due to a temperature change or by non-solvent addition, by pH adjustment, or by the addition of an oppositely-charged polymer. During coacervation of the polymer, droplets of the coacervate adhere to the dispersed phase material then coalease to form a continuous film. Coacervation can take place by a process described as "simple" or "complex" coacervation. Simple coacervation is the process of "salting out" the polymer by salt or nonsolvent, whereas complex coacervation occurs when an oppositely-charged macromolecule is added forming an insoluble complex. Aqueous-based systems have thus far been most widely employed in the coacervation process. The resulting microparticles have sizes range from approximately 1 to 2000 μm.

2.2.5. Solvent Evaporation

Microspheres can be prepared by first dissolving or dispersing active agents in a polymer solution of a single or mixed organic solvent having a low boiling point. This phase is then emulsified in an aqueous phase forming an o/w emulsion. Alternatively, a multiple water-in-oil-in-water (w/o/w) emulsion may also be formed to produce microcapsules. Reduced pressure and/or heat is then often applied to evaporate the organic solvent leaving a film of polymer surrounding each particle. Water-soluble polymer cannot be used in this process. Microparticles of less than 1 μm to as large as 250 μm in size have been reported[22].

2.2.6. Suspension Crosslinking

This is the method of choice for the preparation of protein and polysaccharide-coated microparticles. Microparticles can be prepared by dispersing a polymer solution containing the active agent in an immiscible liquid. The crosslinking is then accomplished either thermally or by the use of a crosslinking agent. Depending on the affinity between the polymer and the two immiscible phases, microcapsules or microspheres can be obtained[23]. Naturally-occurring or preformed synthetic polymers, including agarose, cellulose, albumin, polystyrene and epoxy resin have been employed in this technique. Both submicron (nanoparticles) and larger microparticles can be produced by this method.

2.2.7. Suspension Polymerization

In suspension polymerization, one or more water-immiscible liquid monomers containing a concentration of soluble initiator is suspended as droplets in an inert liquid, usually water. Suitable mechanical agitation is maintained while polymerization is completed to form solid beads or microparticles. Microparticle sizes range from about 50 to 500 µm. Many monomers can be employed in this method, such as styrene, acrylonitrile and vinyl chloride[24].

2.2.8. Emulsion Polymerization

Emulsion polymerization differs from suspension polymerization in that the initiator employed is water-soluble and is located in the continuous aqueous phase. Generally, more vigorous agitation and much higher concentrations of surfactant are employed, as a result of which the droplet size is below 100 µm, and is often less than 1 µm[25]. The most commonly used monomers are styrene, methyl methacrylate and vinyl acetate.

2.2.9. In-situ Polymerization

In this technique, monomer component and catalyst are fed exclusively from either the inside or outside of the core material droplet. Reaction conditions are such that the monomer is soluble while the polymer is not. Thus, the polymerization occurs on the surface of the core material which may be either solid or liquid in this system. This technique is versatile in the actual method applied. For example, the polymerization catalyst can be implanted on a surface of a solid core. Thus, polymerization initiates at this catalytic surface and proceeds to enclose the core material. Another approach involves the separate suspension of drops of core material and monomer in a liquid medium[26]. Most known polymerization reactions can be applied and generally, the resulting particles have a size ranging from about 20 μm to several hundred micrometers.

2.2.10. Interfacial Polymerization

This technique involves two complementary monomers which are in each of two phases. The reaction takes place at the interface between the two liquids while one phase is dispersed in the other. The monomers are usually an organic acid and a compound containing an active hydrogen atom, such as an amine or alcohol[27]. The active agent to be encapsulated is included in the disperse phase. This technique can be employed to prepare microcapsules or microspheres, depending on the solubility of the polymer. Particle size varies from 20 μm to several hundred micrometers. Polyamide, polyurethane and polyurea microparticles have been obtained using this technique.

2.3. Types of Core Materials

Currently, little information is provided in the literature on the microencapsulation of water-soluble compounds. Furthermore, different microencapsulation techniques are applied to core materials of differing water-solubilities. Therefore, it is helpful to differentiate the general techniques into those which are available for water-soluble and those available for water-insoluble materials. These are listed in Table 2.2.

Table 2.2 Microencapsulation techniques available for water-soluble and water-insoluble materials

For water-soluble materials	For water-insoluble materials
pan coating	pan coating
air suspension coating	air suspension coating
spray drying	spray drying
coacervation	coacervation
solvent evaporation	solvent evaporation
suspension crosslinking	suspension crosslinking
in-situ polymerization	in-situ polymerization
interfacial polymerization	emulsion polymerization
	suspension polymerization
	interfacial polymerization

2.4. Design of Controlled Release Microparticles

Microencapsulation is now the most frequently employed method of obtaining sustained and controlled release of chemicals. Except for magnetically or ultrasound controlled systems, otherwise referred to as "triggered release" systems, controlled release devices employ polymer as the rate controlling mechanism. Fabrications of microencapsulated controlled release systems include:

1) Diffusion controlled systems
    a. Reservoir system
    b. Matrix system/Monolithic system
2) Chemically controlled systems
    a. Bioerodible system

b. Pendent chain system

3) Swelling controlled systems

The following examples represent the basic, simplified systems. More complex systems and combinations of more than one mechanism of release (e.g., diffusion plus swelling) are also possible.

2.4.1. Diffusion Controlled Systems

2.4.1.1. The reservoir system:

In this type of system, a core is surrounded by a polymer (Fig. 2.2.) and diffusion of the core material through the polymer is the rate-determining step. The predominant type of polymer used in this system is a non-porous, nondegradable homogeneous polymer film and the release rate is governed by Fick's first law of diffusion.

Figure has been removed due to copyright.

Figure 2.2 Idealized diagram of cross-section of a spherical diffusion-controlled membrane-enclosed reservoir system (taken from R. Langer, Ref. 34).

2.4.1.2. The matrix system

In this system, the agent is distributed, ideally uniformly, throughout a solid nondegradable polymer (Fig. 2.3). As in the reservoir system, diffusion of agent through the polymer matrix is the rate-limiting step. Basically, the same principles which apply to reservoir systems also apply to matrix systems. However, because of the different way in which agent is distributed, the release behaviour of solute in the two systems is not the same. The basic principles of several general cases are considered below.

Case I - Dissolved agent. Diffusion through the polymer

In this case, the initial loading of agent per unit volume is less than the agent solubility in the matrix. Agent diffusion through the polymer occurs via a solution-diffusion mechanism. Baker and Lonsdale[28] have applied two reasonably simple equations to approximate release for different dimensional models.

Case II - Dispersed agent. Diffusion through the polymer

In this case, the initial loading of agent per unit volume is greater than the agent solubility in the matrix and dissolved agent diffuses through a non-porous polymer via a solution-diffusion mechanism. A mathematical model describing this case was put forth by Higuchi[29-30] in 1961, based on Fick's first law of diffusion.

Case III- Dispersed agent. Diffusion through channels

In this case, the initial loading of agent per unit volume is greater than the agent solubility. However, the mechanism in this case involves leaching of solute through intergranular openings in the matrix after dissolution as well as diffusion from the polymer matrix. T. Higuchi[30] has treated this case in much the same way as for a non-porous system in case II with the only difference being the introduction of two parameters i.e., porosity and tortuosity. An extensive series of studies done by Desai and W. Higuchi have been conducted to examine factors affecting release from a case III system for different types of polymer[31-33].

Figure has been removed due to copyright.

Figure 2.3 Idealized diagram of the cross-section of a spherical diffusion-controlled matrix system with dispersed active agent (taken from R. Langer, Ref. 34).

2.4.2. Chemically Controlled Systems

2.4.2.1. Bioerodible system

In this type of system, the drug is distributed, ideally uniformly, throughout a bioerodible polymer prepared essentially as a non-biodegradable matrix system. The same techniques are employed to prepare both types of polymeric systems. However, encapsulated material is released not only by diffusion through the polymer matrix, but the volume of the total bioerodible system also decreases with time. Thus, as the polymer erodes drug is released (Fig. 2.4). This behaviour offers a significant advantage over the non-erodible system in pharmaceutical and medical applications, such as implants, since surgical removal of the device becomes unnecessary.

Figure has been removed due to copyright.

Figure 2.4 Idealized diagram of the cross-section of a spherical bioerodible sphere. The dots outside the sphere represent agent released (although in actuality much of the agent would have diffused further away from the implant) (taken from R. Langer, Ref. 34).

The ideal situation considered by Hopfenberg[35] in which surface erosion is the only factor responsible for agent release is rarely found in practical usage. Mechanisms of degradation of polymer have been proposed by Heller and Baker[36] pertaining to three possible dissolution mechanisms of the polymer: 1) water-soluble polymers made insoluble by degradable crosslinks; 2) water-insoluble polymers solubilized by hydrolysis, ionization, or protonation of pendant groups; and 3) water-insoluble polymers solubilized by backbone cleavage to small water-soluble molecules (Fig. 2.5). These mechanisms may apply in simple straightforward cases, but erosion by a combination of these mechanisms is also possible.

Figure has been removed due to copyright.

Figure 2.5 Schematic diagram of three mechanisms of bioerosion (taken from J. Heller, Ref. 36).

2.4.2.2. Pendent chain system

In this type of system, agent is chemically bound to a polymer backbone and is released by hydrolytic or enzymatic cleavage (Fig. 2.6). The use of these systems have received considerable attention in the design of polymer-drug complexes for short-term use that can reduce toxicity, increase therapeutic efficiency, or be targeted toward specific cells or organs[37-40].

In the pendent chain system, as shown in Fig. 2.6, agent attached to a polymer backbone can be either soluble or insoluble. Soluble backbones are generally used for transport functions such as cell targeting[38-40]; insoluble forms are more desirable for long-term controlled-release implants. The backbone may also be biodegradable or non-biodegradable. Besides, the agent itself can be attached directly to the polymer or it can be attached via a spacer group which can be used to affect the rate of release and the hydrophilicity of the system[38].

Figure has been removed due to copyright.

Figure 2.6 Idealized diagram of a chemically controlled pendent chain agent delivery system. The agent could be connected to the polymer backbone as shown or could be coupled to a spacer group attached to the polymer bachbone (taken from R. Langer, Ref. 34).

These pendent chain systems offer a very important advantage over other release systems in that over 80% by weight of the total delivery system is the agent itself. So far, they are still in their infancy from the standpoint of developing long-term, zero-order controlled-release implants for *in vivo* use.

2.4.3. Swelling Controlled System

In this system, the agent is dissolved or dispersed within a polymer matrix but is not able to diffuse through the matrix, e.g. the particles are too large. Environmental fluid is then imbibed by the matrix, causing it to swell and the drug contained in that part of the polymer is then able to diffuse through the polymer (Fig. 2.7). Thus, the release rate is determined by the rate of diffusion of ambient fluid into the polymer and diffusion of the particles through pores formed within the polymer as a result of swelling. In this case, the rate of release is equal to the product of the surface area and a rate constant corresponding to the rate of advance of the boundary separating the outer depleted zone (swollen and containing no drug) from the central core (unswollen and containing drug). Hopfenberg and Hsu have performed model experiments and found that the rate constant can be calculated from either kinetics of release or microscopic measurements[41]. However, the description of swelling controlled release systems are still largely at a conceptual stage of understanding.

Figure has been removed due to copyright.

Figure 2.7 Idealized diagram of the cross-section of a spherical swelling controlled matrix (taken from R. Langer, Ref. 34).

2.5. Kinetics of Agent Release

Currently, complete mathematical analysis is not available for every single controlled release system. However, several mathematical models commonly employed to describe how an agent is released will be discussed.

The release rate of a solute through an isotropic medium by passive diffusion is governed by Fick's first law of diffusion. Thus, the flow of mass or flux for reversible diffusion is proportional to the concentration gradient of the diffusing species across the region of interest and is described by:

$$J_A = -CD_A \nabla x_A \qquad (2.1)$$

where J_A is the flux of A, C is its molar concentration, D_A represents its diffusion coefficient or mass diffusivity in the medium and x_A is its mole fraction. Accordingly, A diffuses in the direction of lower mole fraction of A.

When Fick's first law is applied to a controlled release system where a single species diffuses across a homogeneous polymeric membrane from a donor reservoir to a perfect sink, where diffusion is considered only in one direction, Eq.(2.1) can be expressed by:

$$\frac{dM}{dt} = -KDS\frac{dC_m}{dX} \qquad (2.2)$$

where dM/dt is the rate of release of the diffusing molecule, D is the diffusion coefficient in the membrane, K is the partition coefficient between the polymer membrane and the aqueous environment, S is the surface area of the membrane, C_m is its concentration in the membrane on the reservoir side and dC_m/dX is the concentration gradient across the membrane. Fig. 2.8 shows a schematic diagram of concentration gradient across an ideal isotropic polymeric membrane under steady state conditions.

Figure has been removed due to copyright.

Figure 2.8 Concentration gradient across an ideal isotropic membrane. Note that the concentrations of solute immediately inside and outside the membrane are not equal because of the preferential partitioning of the solute in the solvent (K<1). $C_m(h)$ and $C_m(l)$ are the membrane solute concentrations at the membrane-bulk solution interface (taken from P. B. Deasy, Ref. 10).

2.5.1. Zero-order Release Kinetics

If the thermodynamic activity of the diffusing substance which is in a reservoir systems, is maintained constant in a polymeric device for a period of time during its release, (such as in a microcapsule), then the steady-state release rate for a spherical device is given by

$$\frac{dM}{dt}=4\pi DK\Delta C_m\frac{r_o r_i}{r_o-r_i} \qquad (2.3)$$

where ΔC_m represents the difference in drug concentration between solutions on either side of the membrane, r_0 and r_i are the outside and inside radii of the microcapsule, respectively. If all parameters on the right-hand side of Eq.(2.3) remain constant, the release rate follows constant or zero-order release. Thus, the rate of release of core material decreases with an increase in the coating thickness

$(r_o - r_i)$. However, by increasing the thickness of the coat or wall material, i.e. increasing r_o only, $dM/dt \rightarrow 4\pi DK\Delta C_m r_i$. When r_o/r_i exceeds a value of 4, further increase in device size for a fixed-core radius does not significantly change the release rate[28].

In practice, zero-order release kinetics can be maintained as long as saturated solution in the presence of excess solid agent exists in the reservoir in order to maintain a constant thermodynamic activity.

2.5.2. First-order Release Kinetics

If the thermodynamic activity of the core material in a microcapsule does not remain constant either because, initially, excess solid was not present in the device or because only a saturated or unsaturated solution of agent was encapsulated, then the rate of release will fall exponentially as the concentration decreases with time. The release is then described by first-order kinetics. However, many microcapsules, particularly those produced by coacervation procedures, do not follow the expected reservoir-type kinetics but instead follow release kinetics according to the Higuchi model.

Mathematical derivations of the release kinetics from a polymer matrix of different geometries have been studied by Baker and Lonsdale[28], and Deasy[10]. Because of the many mathematical calculations involved, only the final equations are given here. Thus, for spherical devices:

$$M_{it}=M_{tot}\exp\frac{[-2\pi(r_i^2+r_o^2)DKt]}{(r_o-r_i)V_i} \tag{2.4}$$

$$\frac{dM_{it}}{dt}=\frac{-M_{tot}2\pi(r_i^2+r_o^2)DK}{V_i(r_o-r_i)}\exp\frac{-2\pi(r_i^2+r_o^2)DKt}{(r_o-r_i)V_i} \tag{2.5}$$

where M_{it} is the mass of agent remaining at any time in the reservoir, M_{tot} is the total agent in the system and V_i is the volume of the internal reservoir. Exponential decline in drug release from microcapsules into an aqueous medium has been reported by many researchers[42]. Eq.(4) can be simplified to

$$\log\frac{M_{it}}{M_{tot}}=\frac{-k' t}{2.303} \tag{2.6}$$

where

$$k'=[\frac{-2\pi(r_i^2+r_o^2)DK}{(r_o-r_i)V_i}] \tag{2.7}$$

Assuming that k' is a constant, plotting the logarithm of percent agent remaining against time, k' can be determined from the slope and hence, it is referred to as the first-order rate constant.

2.5.3. Matrix Release Kinetics. The Higuchi Model

The release kinetics for case II and case III in a matrix system, as mentioned earlier, are described by the well-known Higuchi model, in which release of agent from the device is a linear function of the square root of time. In case II, the initial loading of agent per unit volume is greater than the agent solubility in the matrix. In this case, the agent diffusing through the non-porous polymer is replaced by agent which originates from dissolution of dispersed solid particles. This model has been experimentally supported by both microscopic and kinetic studies for low molecular weight drugs of low solubility[28,43-44]. A schematic diagram describing agent released from a slab of cross-sectional area A, with associated concentration gradients, is shown in Fig. 2.9. The release of agent, as mathematically derived originally by Higuchi, from a monolithic slab is also often used to approximate release from irregularly-shaped microparticles, such as those prepared from coacervation and is given by,

$$\frac{dM}{dt}=\frac{A}{2}\left[\frac{DC_s(2C_{tot}-C_s)}{t}\right]^{1/2} \qquad (2.8)$$

which upon integration gives

$$Q=\frac{M}{A}=[DC_s(2C_{tot}-C_s)t]^{1/2} \qquad (2.9)$$

where Q is the amount of agent released after time, t, per unit of exposed area, C_{tot} is the total amount of agent present in the matrix per unit volume, and C_s is the solubility of the agent in the matrix. It is assumed that $C_{tot} \gg C_s$, that the noninteracting, uniformly dispersed drug particles are much smaller in diameter than the thickness of the matrix, and that perfect sink conditions prevailed in the release medium. These equations are only valid as long as the agent concentration remaining in the polymer still exceeds its solubility. Thus, at late time periods the model and the equations are no longer valid.

Figure has been removed due to copyright.

Figure 2.9 Diagram of agent distribution and concentration gradients within an idealized rectangular or slab matrix (monolith) as a function of time. The dark black lines represent barriers through which the active agent cannot penetrate. This diagram is the basis of the Higuchi Model (taken from T. Higuchi, Ref. 29 and 30).

Assuming that D, C_s, and C_{tot} remain constant, Eq. 2.9 may be reduced to

$$Q=k_1t^{1/2} \qquad (2.10)$$

where k_1 is a constant. Jalsenjak et al.[45], Madan[46], and many others have reported that agent release from microcapsules produced by coacervation was proportional to $t^{1/2}$.

Higuchi subsequently presented the following equation for steady-state release from the planar surface of a granular-type matrix (case III)[30]:

$$Q=[\frac{D_w\phi}{\tau}(2C_{tot}-\phi C_{sw})C_{sw}t]^{\frac{1}{2}} \qquad (2.11)$$

Where D_w is the diffusion coefficient of the agent in the permeating fluid, ϕ is the porosity of the leached portion of the matrix, τ is the tortuosity factor of the capillary system and C_{sw} is the solubility of the agent in the permeating fluid. All of the same assumptions were made as for case II except that in this case, release is governed by diffusion through channels or pores in the polymer matrix rather than by a solution-diffusion mechanism in the polymer itself. As the tortuosity factor is often assumed to be about equal to 3, Eq. 2.11 is valid provided that C_{tot} is greater than C_s by a factor of 3-4, (Eq. 2.9).

2.6. General Safety Considerations

Microencapsulation techniques have raised some concerns because of the chemicals and solvents used which can be toxic or hazardous. Thus, because of increasing applications of microencapsulation, the pros and cons of microencapsulated products with respect to the environment and to public health are briefly discussed.

2.6.1. Environment Concern

In the past decade, there has been arguments of the absolute need for pesticide chemical usage in agriculture versus the desire for a quality environment free of toxic materials. Microencapsulation technology has offered a solution to this problem by substantially decreasing the amount of pesticide added to the environment over a given period of time and, most importantly, by enabling the substitution of short lived, nonpersistent materials to be used as opposed to those having an undesirably long exposure to the environment. Microencapsulated fertilizing material, for example, would be relatively unaffected by rainfall or ground water wash-out because the size of the polymeric particle would control the level of lateral or downward movement in the soil. As a result, marked reduced fertilizer permeation and loss to the soil, thereby reducing the poisoning of water supplies and concomitant loss of fish and shellfish life[47], are positive outcomes of microencapsulation.

With the large volumes of organic solvent which have been involved in some of the microencapsulation processes, the use of aqueous-based coatings has rapidly gained in popularity. Thus, studies have shown that inert water-soluble celluloses, such as hydroxypropylcellulose and hydroxypropylmethylcellulose, are useful coating materials. Also, because of the growing concern over general environmental pollution by plastics, the biochemical degradation of these polymers will be given increased attention.

2.6.2. Public Health Concern

In the agricultural industry, microencapsulation also reduces the health hazard to those handling the toxicants. This has been particularly beneficial in the use of pesticides since controlled release has resulted in decreased dosages and possible undesirable linkages to the food chain.

It is apparent that the choice of film-former for a particular application is dependent on the toxicity of the polymer, particularly if it is to be used in humans. Orally consumed polymers are rarely absorbed because of their large molecular weight, and hazards associated with their use are often related to their residual monomer and catalyst content. Any process or material involved in the application of microencapsulation in foods, pharmaceutical or veterinary products have to be approved by federal regulatory agencies, such as the HPB (Health Protection Branch) or the FDA (Food and Drug Administration). The approval requirement also extends to methods of solvent removal, conditions of storage, and methods of handling, etc.

The development of microparticulate systems as drug carriers using biodegradable polymers has been extended to parental use. Microencapsulated products known as nanoparticles intended for intravenous therapy have also been developed. However, it is sometimes found that these nanoparticles tend to be extensively phagocytized by cells of the reticuloendothelial system, which may cause unwanted accumulation in organs such as liver, spleen and lungs.

2.7. Industrial Applications

2.7.1. Agricultural

During the 1960s, many persistent pesticides were phased out because of environmental and toxicological problems. They were usually replaced by pesticides that had very short persistence in the field but much higher mammalian toxicity than the compounds which they replaced. The application of microencapsulated pesticides, as a means of controlling the release of biodegradable and/or short-lived pesticides in the required amounts over a period of time, appears to offer an ideal solution to these problems. Figure 2.10 shows the relationship between the level of application and duration of action for conventional formulations (curve A) and for controlled-release formulations (curve B). In preparing Fig. 2.10, Lewis and Cowsar assumed that the availability half-life of the pesticide was 15 days and that the minimum effective level was 1 g/acre[48].

Figure has been removed due to copyright.

Figure 2.10 Relationship between the level of application and the duration of action of conventional and controlled release formulations (taken from D. Lewis et al., Ref. 48).

Microcapsules containing pesticides in the size range of 10 to 100 μm are generally most useful because they yield increased residual activity and have higher efficiency. Microcapsules having these properties can be easily prepared by many microencapsulation techniques. The choice of method depends mainly upon the nature of the pesticide and the release-controlling membrane. Common polymeric wall materials have included polyamides, polyesters, polyureas, cellulose, and gelatin.

Currently, the most commonly employed technique is interfacial polymerization[49]. Active ingredients that are best encapsulated by this method are organic liquids of very low water solubility containing no functional groups that could react with the encapsulating material. Many of the most widely used pesticides fall into this category.

The first microencapsulated product sold in the U.S. for agricultural use was PENNCAP-M® INSECTICIDE, containing methyl parathion, manufactured by the Pennwalt Corporation[50-51]. This short-acting pesticide was encapsulated in a polyamide (nylon) wall material. The microcapsules are about 30 μm in diameter, and contain about 80% of the active agent by weight. This product, which has received registration with the Environmental Protection Agency, exhibits decreased toxicity and longer activity when compared with the conventional application of the insecticide.

The Wurster air suspension process has also found applications in this area. An example of a unique product utilizing the concept of sustained release is cotton seed which is coated with a polymer containing DiSyston®. Prior to developing this product, cotton seed was treated by applying the insecticide directly onto the seed. This resulted in significant phytotoxicity to the seed and reduced germination and vigor. With untreated seed, germination and vigor were good, but the young seedling was very susceptible to insect predation. With the formulation of this product, several of the problems of the insecticides are avoided and a few other benefits are gained[52-53].

2.7.2. Pharmaceutical

It is well-known that microencapsulation can provide a means to prepare SR formulations and the use of microencapsulation for the production of SR dosage forms in pharmaceutics has been widely employed in the last 30 years, since its successful introduction by Smith, Kline and French in the early 1950s.

Investigators continually search for new drugs to help solve biological and medical problems. Usually, the effectiveness of chemotherapy is dependent on the amount available and the dose frequency. Normal administration, other than intravenous, usually results in peaks and valleys of drug levels in biological fluids. This is not only inefficient drug administration but can lead to undesirable side effects and subpotent concentrations required in therapeutics. The development of new, improved sustained release (SR) formulations is a means of providing more effective products for new as well as old drugs at a cost considerably less than that required to develop a new drug. Thus, many of the new drug products available today are SR oral dosage forms based on the microencapsulation principle.

The ideal SR formulation for many drug therapies is one which releases the drug at a constant rate, which also provides a constant rate of absorption and produces sustained therapeutic concentrations for the entire dosing interval. Ideally, a SR formulation is a means to improve therapy by maintaining uniform steady-state plasma concentrations, by reducing the ratio of maximum and minimum plasma concentrations (C_{max}/C_{min}) in the plasma concentration-time profile.

The physicochemical properties of a drug, including stability, solubility, partitioning characteristics, charge, and protein binding, play dominant roles in the design and performance of a SR product. For instance, a drug with a very high water solubility or molecular weight over 500 is reported to be comparatively difficult to formulate into SR microencapsulated products[10]. In addition, the properties of polymers used must be taken into account for any specific application. Other aspects of development of microcapsules for oral delivery are, in part, the subject of this thesis.

2.7.3. Enhanced Oil Recovery Processes

Microencapsulation has found extensive use not just in agricultural and pharmaceutical applications, but in other industries as well, and developments using these techniques are expanding each year. The idea of using microencapsulated products to augment enhanced oil recovery (EOR) processes is relatively new and so far, only a few studies have been performed.

The history of injection of pressurized water into oil reservoirs as a means of enhancing petroleum recovery dates back to the early part of the twentieth century. More than 50% of Alberta's light oil is produced by "waterflooding" techniques. Clean water is injected at one or more wells to push the oil through the reservoir to nearby production wells where oil is pumped to the surface.

Experience shows that the water injected eventually manages to find a small path or channel to a producing well thus bypassing a significant portion of the reservoir. Typically, the oil is much more viscous than the water and thus, the amount of water produced each day soon exceeds the amount of oil produced. It has been reported that conventional oil production methods recover only from 8 to 30% of the total oil present in a petroleum reservoir[54].

Recently, Costerton and his research associates have developed a microbial process whereby slime producing bacteria, isolated from produced oilfield water and fed by a continuous nutrient supply, are used to plug high permeability water channels in oil zones[55]. Vegetative bacteria were injected into model porous media cores and plugging was caused by production of exopolysaccharides called glycocalyx[56], commonly referred to as slime. In order to achieve slime plugging in the very small water channels, the requirements are nonadhering properties, a size less than 1 μm, and rapid bacterial growth and slime production.

A type of bacterium isolated from the produced water (water coproduced with oil), identified as *Klebsiella pneumoniae* was found to meet all the criteria[57-59]. Bacteria of this type shrink in size, becoming very small when starved, to 0.1 to 0.3 μm and are called "ultramicrobacteria" or UMB. A high-energy source nutrient which facilitates the transition from a UMB state to a vegetative, slime-producing state is Brain Heart Infusion Medium (BHIM).

The practice of injecting materials into hydrocarbon reservoirs to effect enhanced oil recovery relies upon the placing of these materials at target sites to achieve either widespread or specific area coverage. Factors such as reservoir heterogeneity, chemical and physical interactions between the injected fluids (e.g. nonideal plugging, piping corrosion and precipitates) and reservoir components work against ideal placement by influencing the flow of the injectant or expending the injectant before target coverage is achieved. Therefore, microencapsulation of BHIM may provide a means to overcome nonideal placement tendencies, thereby avoiding overdosage and, additionally, provide for a sustained release of BHIM over time and/or a delayed release until conditions for release are attained.

Exxon Research & Engineering has been granted the first patents covering the techniques involving the introduction of microparticles and micocapsules into hydrocarbon reservoirs to achieve the delayed and controlled release of oil field chemicals[60-61]. These polymeric particles can be used in conjunction with water-soluble or water-insoluble materials, but their size ranged from 50 μm to 1 mm. This limits the introduction of these into reservoir fractures, wellbores, flowstreams or vessels.

Recently, Conoco Inc. has been granted two patents involving techniques in this area as well[62-63]. Polymeric particles and microcapsules containing water-soluble or water-insoluble materials were prepared by condensation or co-condensation techniques. The microparticles dissolve over a period of time and release the oil field chemical. Again, the size range was large, varying from 1 to 900 μm.

CHAPTER III

3. AIMS AND SCOPE OF THE THESIS

3.1. Microencapsulation of A Nutrient (BHIM)

3.1.1. Aim

The aim of this research was microencapsulation of a high energy nutrient (Brain Heart Infusion Medium), used to stimulate in-situ microbial enhanced oil recovery. Ideally, the microcapsules should meet the following criteria:

1. a mean microcapsule size of less than 1 µm in diameter.
2. robustness of the microcapsules during injection.
3. delayed release of the microcapsule contents for at least 24 hours.
4. sustained release of the microcapsule contents for approximately 30 days.
5. a suitable encapsulation efficiency and yield.

The first of the criteria is based on the expectation that 1.0 µm sized particles suspended in fluid are able to penetrate porous media with a permeability of 500 millidarcies. Hence, microcapsules of BHIM in the order 1.0 µm mean diameter can be co-injected with UMBs and may overcome nonideal placement tendencies. Robustness of the microcapsules is essential in order to withstand rupturing under stress conditions during pressurized injection. Delayed release of the nutrient provides the opportunity to co-inject microencapsulated nutrient and microbes in one operation, avoiding formation of a biomass skin plug until the required quantities have been injected, and ensuring intimate co-placement of both in the pore spaces of the porous media. Sustained release of the nutrient would ensure that the microbial activity stimulated by the nutrient would be prolonged. Finally, a suitable encapsulation efficiency and yield would provide a sufficient amount of BHIM released during the process at reasonable cost.

A review of literature indicated that procedures which enable the formation of small microcapsules (≈ 5 μm) and which can be used for water-soluble agents are very limited. Basically, they include a) spray drying[64], b) in-situ polymerization[6], and c) interfacial polymerization[65]. Microcapsules are the most likely to give the desired characteristics since a large fraction of the microcapsule weight of agent is attainable.

3.1.2. Objectives of Research On SR Microcapsules of BHIM

1. to prepare microcapsules of BHIM using the proposed techniques and polymer compatible with BHIM and having a mean size of about 1 μm.
2. to optimize the formulation with respect to BHIM encapsulation efficiency and size distribution.
3. to characterize the microcapsules in terms of particle size and surface morphology by means of SEM.
4. to measure the release of BHIM from the microcapsules.
5. to study the effect of BHIM microcapsules on the growth rate of UMBs.

3.2. Microencapsulation of Antihistamine Drugs

3.2.1. Aim

The aim was to prepare sustained release formulations of antihistamines for oral delivery in order to prolong their therapeutic effects while minimizing unwanted side effects associated with peak plasma levels after typical oral administration (i.e. dose dumping). Microencapsulation techniques have been employed to encapsulate two water-soluble antihistamines, namely diphenhydramine HCl and dimenhydrinate having water-solubilities of 1g/ml and 1g/95ml, respectively.

Diphenhydramine HCl and its chlorotheophylline salt, dimenhydrinate, are H_1 receptor antagonists belonging to the ethanolamine-type antihistamine drugs that block H_1 receptors. After administration, antihistamines are widely distributed throughout the body and the central nervous system (CNS), metabolized by hepatic enzymes and excreted in urine. Each has a relatively short elimination half-life. The terminal elimination half-life of diphenhydramine HCl has not been fully elucidated, but appears to range from 2.4-9.3 hr in healthy adults[66]. A half life of 5.3 hr has been reported for dimenhydrinate[67].

The nonspecificity of H_1 receptor antihistamines often results in sedation and other unwanted side effects and is positively correlated with plasma concentration (70 ng/ml in plasma). Thus, these antihistamines have properties which make them good candidates for sustained release.

3.2.2. Objectives of SR Microparticle Formulation of Antihistamines

1. to prepare encapsulated microparticles of water-soluble drugs exemplified by diphenhydramine HCl and dimenhydrinate. The non-biodegradable polymers Eudragit RS 100 and ethylcellulose were selected because of their inert properties and their versatility as coating materials using different microencapsulation techniques, including coacervation and solvent evaporation.
2. to evaluate size and morphological characteristics of the produced microparticles.
3. to determine the release kinetics of antihistamine from the microparticles and apply the appropriate mathematical models in order to gain some insight into the kinetic mechanisms involved.

CHAPTER IV

4. EXPERIMENTAL

4.1. Microencapsulation of Brain Heart Infusion Medium

4.1.1. Preparation of PMMA Microcapsules by Spray Drying Technique

4.1.1.1. Materials

Poly(methyl methacrylate) (PMMA) was obtained from Fisher Scientific Company (Fair Lawn, New Jersey). Brain Heart Infusion Medium (BHIM, dehydrated), an energy-rich infusion medium recommended for organisms generally considered difficult to cultivate, was obtained from Difco Laboratories (Detroit, Michigan). All other reagents and solvents were at least reagent grade.

4.1.1.2. Preparation of spray-dried BHIM powder

An aqueous solution of 4% w/v BHIM was spray-dried (Büchi Mini Spray Dryer-Model 190) to reduce particle size and form more uniform particles of the BHIM powder before microencapsulation. The process parameters were as follows: inlet temperature (200^{o}C); outlet temperature (95-100^{o}C); aspirator setting (5); pump setting (3); spray flow (800 NLh^{-1}, NL = normliter) from a 0.5 mm spray nozzle. The spray-dried product was collected in the collection chamber, modified to receive the product in a small (50 ml) beaker.

4.1.1.3. Preparation of BHIM-loaded PMMA microcapsules

PMMA (2.0, 2.4, 2.8 or 3.2% w/v) was dissolved and spray-dried BHIM powder (2.0% w/v) was dispersed in 25 ml methylene chloride containing 5% v/v Span 80 as emulsifier. The dispersion was sonicated with a titanium microtip

(Model W-375, Heat System-Ultrasonics, Inc.) for 2 min at 40 W prior to microcapsule preparation using the spray-dryer. The process parameters in this instance were as follows: inlet temperature (70°C); outlet temperature (40-45°C); aspirator setting (5); pump setting (4); spray flow (800 NLh^{-1}) from the 0.5mm spray nozzle. Controls experiments were also carried out under similar experimental conditions in the absence of BHIM powder. The dried products were collected as before and stored in a desiccator until ready for use.

4.1.1.4. Microscopic studies

Samples of raw (untreated) BHIM powder, spray-dried BHIM powder, and PMMA microcapsules were prepared by coating the sample with gold vapor under high vacuum (work done by Dr. Chen, SMRI, U of A). Observations of size distributions and particle surface morphology were recorded from SEM micrographs (Philips SEM 505, Holland).

4.1.1.5. Release studies

Release studies of BHIM from PMMA microcapsules were carried out by suspending 100 mg PMMA microcapsules in 500 ml distilled water (23°C) in a 1000 ml conical flask and stirring at setting 100 upm (unit per minute, Ikamag Ret-G, stirring hot plate, range 0-800 upm) using a 38-mm octagonal stirring bar. Samples were withdrawn at various time intervals and the amount of BHIM released was quantitated using a modified Lowry protein assay[68], measuring absorbances at 750 nm (Beckman Model 25 Spectrophotometer) from which concentrations were determined using a calibration curve.

4.1.2. Preparation of PMMA Microcapsules by In-situ Polymerization

4.1.2.1. Materials

Methyl methacrylate (Aldrich Chemical Co. Milwaukee, WIS) was purified from polymerization inhibitors by distillation before use. BHIM was obtained from Difco Laboratories. Potassium persulfate ($K_2S_2O_8$) was obtained from Caledon Laboratories Ltd. (Georgetown, Ontario) and ferrous sulfate ($FeSO_4$) was obtained from J. T. Baker Chemical Co. (Phillipsburg, N. J.). All other chemicals or solvents were of analytical grade.

4.1.2.2. Preparation of PMMA microcapsules

The water-soluble initiator, potassium persulfate (1%, 2.5%, 5% w/v), was first dissolved in 1 ml 40% w/v sterile BHIM solution. This aqueous solution was then mixed with 15 ml cyclohexane:chloroform (4:1 v/v) containing Span 85 (6.67% v/v) with vigorous stirring. After 5 min, 2 mL of methyl methacrylate was added under a N_2 atmosphere. The temperature was maintained for 6 hr at 80°C to generate the sulfate radical or 1 ml of $FeSO_4$ solution (1-5% w/v) was added, and the reaction carried out for 4 hr at room temperature (23°C) while stirring.

The PMMA microcapsules which formed were centrifuged at 110 x g for 5 min. The microcapsules were then dispersed in 10 ml of aqueous 50% v/v Tween 20 solution following which 40 ml distilled water were added. This dispersion was centrifuged for 20 min at 1,753 x g, the supernatant removed, and the microcapsules again resuspended in 20 ml of distilled water.

4.1.2.3. SEM studies

A sample of the PMMA microcapsule dispersion prepared above was dried in the air, then coated with gold vapor under high vacuum (work done by Dr. Chen, SMRI, U of A) and SEM micrographs recorded (Philips SEM 505, Holland). The observed surface morphology and size of the microcapsules were recorded from the SEM micrographs.

4.1.3. Preparation of Polyamide Microcapsules by Interfacial Polymerization

This microencapsulation method was based on interfacial polycondensation first studied in detail by Morgan and Kwolek[69]. The electrocapillary emulsification technique[70] was applied in this study to obtain a small particle size. Two water-soluble monomers, L-lysine and piperazine, were used for comparison in this study.

4.1.3.1. Materials

Brain Heart Infusion Medium (dehydrated) was obtained from Difco Laboratories. L-lysine (L-2,6-diaminohexanoic acid) monohydrate and piperazine anhydrous (hexahydropyrazine) were obtained from Sigma Chemical Co. (St-Louis, MO). All other chemicals and solvents were at least reagent grade.

4.1.3.2. Preparation of BHIM solution

2 g or 4 g of BHIM were dissolved in 10 ml of demineralized, distilled water then sterilized by autoclaving (121°C, 15 psi) for 15 min. 0.73 g L-lysine (or 0.70 g piperazine) and 0.66 g sodium carbonate were then dissolved in the solution.

4.1.3.3. Preparation of polyamide microcapsules

BHIM-loaded polyamide microcapsules were prepared by the electrocapillary emulsification technique originally described by Arakawa and Kondo[65,71]. Fig. 4.1 shows the schematic diagram of the apparatus used for electrocapillary emulsification. The aqueous phase (A) in a syringe (D) was introduced into the oil phase (B) at a fixed rate using a syringe pump through a stainless steel needle (E), which was also the anode of the electrical circuit. The anode and a platinum electrode (C) (cathode) in the oil phase were connected in series to a variable dc power supply (F), the potential of which was measured by a voltmeter (V). The oil phase was gently stirred during the addition of the aqueous phase by a magnetic stirrer (G).

Figure has been removed due to copyright.

Figure 4.1 Schematic diagram of the apparatus for electrocapillary emulsification (taken from M. Arakawa and T. Kondo, Ref. 65).

The aqueous phase described above was dispersed as very fine droplets into 50 ml cyclohexane:chloroform (3:1 v/v) containing terephthaloyl chloride (0.04 M), tetraethylammonium chloride (1.5×10^{-4} M), and sorbitan trioleate (5% v/v). Electroconductivity was conferred to the oil phase by the presence of the tetraethylammonium chloride. The BHIM solution (1 ml) was introduced by means of a syringe, pumped at a rate of 0.015 ml/min (syringe pump, model 355, Sage instruments) to 50 ml of the oil phase in a 100 ml beaker. A potential difference of 850 volts was applied at an electrode separation distance of approximately 5 mm while the oil phase was being gently stirred at setting 600 upm (Ikamag Ret-G) using a 25-mm octagonal stirring bar. The applied potential was set above the critical potential difference for dispersion, resulting in the formation of a shower of fine droplets which were immediately emulsified to form a w/o emulsion. The applied potential was positive on the aqueous phase side with respect to the oil phase.

At the surface of each droplet, polycondensation took place between the amide (L-lysine or piperazine) and terephthaloyl chloride to form a poly(L-lysine terephthaloyl chloride), (PLT), or poly(piperazine terephthaloyl chloride), (PPT), membrane. The HCl formed as a reaction by-product was neutralized immediately by the alkali in the aqueous phase. The polyamide microcapsules which formed were centrifuged at 110 x g for 5 min, separated, then completely dispersed in 10 ml of aqueous 50 %(v/v) Tween 20 solution, followed by a further addition of 40 ml distilled water. This dispersion of microcapsules was then centrifuged for 20 min at 1,753 x g, the supernatant removed, the microcapsules resuspended in 50 ml of distilled water, then recentrifuged at 1,753 x g for 20 min. Precautions were taken to ensure that all glassware and demineralized, distilled water were sterilized by autoclaving before use.

4.1.3.4. SEM studies

Polyamide microcapsules suspended in 50% Tween 20 solution were dried and coated with gold vapor under high vacuum (work done by Dr. Chen, SMRI, U of A). Again, size distributions and surface characteristics of the observed microcapsules were recorded on SEM micrographs (Hitachi SEM S-2500).

4.1.3.5. Characterization of PLT and PPT microcapsules

BHIM-loaded microcapsules obtained from each single batch were dispersed in 50 ml of distilled water to form a stock solution. 10 ml of the microcapsule suspension was transferred to a vial and autoclaved for 20 min. This was centrifuged for 6 min at 15,909 x g. 1 ml of the supernatant was removed and analyzed for BHIM. In addition, 10 ml of the polyamide microcapsules were filtered (Whatman filter No. 5) under vacuum and the weight of microcapsules was determined after drying in an oven at 40°C for 48 hr. Encapsulation efficiency, fraction of BHIM encapsulated, and yield of microcapsules were determined.

4.1.3.6. Release studies of polyamide microcapsules

Release studies were carried out at room temperature (23°C) and 40°C. A sample of the microcapsule suspension (1.4 ml) was centrifuged (15,909 x g, 6 min) at various time intervals, and the supernatant analyzed for BHIM.

4.2. Microencapsulation of Dimenhydrinate

4.2.1. Materials

Dimenhydrinate and Span 80 were obtained from Sigma Chemical Co. (St. Louis, MO). Ethylcellulose N-100 (viscosity of 5% w/v solution in 80:20 v/v toluene-ethanol = 100 cP, ethoxy content 48.0-49.5%) was obtained from Hercules Co. (Wilmington, DE). All other chemicals and solvents were of analytical grade. Demineralized, distilled water from a Milli-Q Plus water purification system was used to prepare the dissolution media.

4.2.2. Preparation of Microparticles

The microencapsulation of a water-soluble drug employing an alcohol-in-oil emulsion was carried out using a methodology similar to that of Huang et al[72]. Exactly 0.3, 0.9 and 1.5 g of dimenhydrinate were dissolved in 25 ml of 95% ethanol containing 1.2% ethylcellulose, yielding compositions of polymer:drug of 1:1, 1:3 and 1:5, weight ratio, respectively. A thin stream of the resulting solution (6 ml) was delivered to 90 ml of heptane:light mineral oil (1:3) v/v containing 1 % Span 80 at 32°C (Ikamag Ret-G stirring hot plate) to enhance dispersibility of the droplets and stirred at 300 rpm (Canlab high torque stirrer equipped with a Nalgene stirrer of 44 mm-blade diameter) for 4 hr. During this period, the alcohol completely evaporated. The microparticles which formed were filtered, washed three times with 50 ml n-hexane, then allowed to dry in a desiccator under reduced pressure.

4.2.3. SEM Studies

Scanning electron microscopy (Hitachi SEM S-2500) was again used under the same conditions as before to examine the morphological features and size distribution of the microparticles.

4.2.4. Size Analysis of Microparticles

Detailed studies of the size distributions in the various batches was carried out by sieve size analysis. The different sizes in a batch were isolated by sieving using a range of U.S. standard sieves and the amounts retained on different sieves were weighed. Sieve size fractions (% w/w) and cumulative per cent less than maximum of the stated size were calculated.

4.2.5. Determination of Dimenhydrinate Loading

The drug content of 10 mg of microparticles was determined by u.v. spectroscopy at 276 nm (Beckman Model 25 Spectrophotometer) of a solution in 95% ethanol. The presence of ethylcellulose did not interfere with the analysis of dimenhydrinate.

4.2.6. Release Studies

Release studies of dimenhydrinate were conducted using a spin-filter dissolution test apparatus[73] (Magne-drive, Clow Coffman Industries, Kansas) equipped with a 1-micron nominal porosity, stainless steel filter screen. The spin filter was rotated at 100 rpm in 500 ml of pH 7.4 phosphate buffer at 37°C. 10 mg of a sieved sample (40/60 mesh) of microparticles were dispersed in the release medium, which was circulated continuously using a peristaltic pump (Gilson Miniplus 2) through a microcell in the spectrophotometer, and concentrations of dimenhydrinate were determined as a function of absorbance. All determinations were carried out in triplicate and averaged.

4.3. Microencapsulation of Diphenhydramine HCl

4.3.1. Ethylcellulose Microcapsules

4.3.1.1. Materials

Ethylcellulose N-100 (viscosity of 5% w/v solution in 80:20 v/v toluene-ethanol = 100 cP, ethoxy content 48.0-49.5%) was obtained from Hercules Co. (Wilmington, DE). Eudragit RS 100 was a gift from Rohm. Tech. Inc. (Malden, MASS). Diphenhydramine HCl and polyisobutylene (PIB, M.W. 380,000) were obtained from Aldrich Chemical Co. (Milwaukee, WIS). All other chemicals and solvents were at least reagent grade.

4.3.1.2. Method of preparation

The ethylcellulose microcapsules were prepared by a modified phase separation method described by S. Benita[74]. Sieved-sized (250-425 μm) diphenhydramine HCl (0.60g) was added to 20 ml of 3% w/v PIB and 4%-16% w/v ethylcellulose N-100 in cyclohexane in a 100 ml three-necked flask and the reaction carried out while stirring at 200 rpm (Canlab high torque stirrer, equipped with a 5-cm teflon blade propeller) at 80°C for 10 min. The system was cooled to 45°C then to 25°C for 15 min to achieve gelsification of the ethylcellulose droplets.

After sedimentation of the microcapsules, the supernatant liquid was decanted and the microcapsules rinsed with three 100-ml portions of cyclohexane to remove any PIB adsorbed at the microcapsule surfaces. The microcapsules were subsequently collected by vacuum filtration (Whatman filter paper No. 1) and stored in a desiccator until ready for use.

4.3.1.3. Optical microscopic studies

Ethylcellulose microcapsules containing diphenhydramine HCl were examined by optical microscopy as a suspension in cyclohexane and characterized according to size, shape and surface characteristics.

4.3.1.4. Diphenhydramine HCL content

The drug content of 250-425 μm microcapsules was determined by dissolving 100 mg microcapsules in 95% ethanol followed by spectrophotometric analysis at 256 nm (Beckman Model 25 spectrophotometer); concentrations were obtained from a standard calibration curve. The presence of ethylcellulose N-100 did not interfere with the analysis of diphenhydramine HCl.

4.3.1.5. Release studies

Release studies of microencapsulated drug were again conducted using a spin-filter dissolution test apparatus. A 200 mg sieve sized sample (40/60 mesh) of microcapsules was dispersed in pH 7.4 phosphate buffered medium at 37°C.

Concentrations of diphenhydramine HCl were determined as a function of absorbance from a calibration curve. All determinations were carried out in triplicate and averaged.

4.3.2. Eudragit RS 100 Microcapsules

4.3.2.1. Method of Preparation

The method of preparation was a modified version of Benita et al.[75]. Sieved-sized (250-425 μm) diphenhydramine HCl (0.45g) was added to 20ml of 6% (w/v) PIB and 8% w/v Eudragit RS 100 in toluene in a 100ml three-necked flask. A solution (60 ml) of 6% w/v PIB in cyclohexane, the non-solvent, was delivered at a rate of 0.5 ml/min (syringe pump, model 341B, Sage instruments) at a constant stirring rate of 200 rpm (Canlab high torque stirrer, equipped with a 5-cm teflon blade propeller) at room temperature. After about 5 min of reaction time stirring was stopped, the microcapsules settled out, the supernatant removed by decantation, and the microcapsules rinsed twice with 100 ml of cyclohexane to remove any residual PIB. Washing was repeated with another 50 ml cyclohexane, then the microcapsules were vacuum-filtered (Whatman filter paper No.1), and finally stored in a desiccator under reduced pressure.

4.3.2.2. Microscopic studies

Microcapsules were examined and characterized by both optical and scanning electron microscopy. Preparation of samples for observation was as previously described.

4.3.2.3. Diphenhydramine HCl content

The drug content of 250-425 μm sized microcapsules was determined by dissolving 100 mg microcapsules in 95% ethanol followed by spectrophotometric analysis at 256 nm (Beckman Model 25 spectrophotometer) and concentrations were obtained from a standard calibration curve. The presence of Eudragit RS 100 did not interfere with the analysis.

4.3.2.4. Release studies

Release studies of microencapsulated drug were again conducted using a spin-filter dissolution test apparatus. A 200 mg sieve sized sample (40/60 mesh) of microcapsules was dispersed in the pH 7.4 phosphate buffered medium at 37°C and concentrations of diphenhydramine HCl were determined as a function of absorbance from a calibration curve. All determinations were carried out in triplicate and averaged.

CHAPTER V

5. RESULTS

5.1. Microencapsulation of BHIM

5.1.1. PMMA Microcapsules by Spray Drying

5.1.1.1. Size and shape analysis by SEM

As shown in Fig. 5.1 A and 5.1 B, spray-dried BHIM powder consisted of spherical particles having a diameter of 1-5 μm compared with 1-80 μm of irregularly-shaped particles of the raw powder. Similarly, spray-dried BHIM-loaded PMMA microcapsules were also spherical (Fig. 5.1 C). However, when blank PMMA microcapsules were prepared, the microcapsules were deformed with concave depressions presumably from collapse of the microcapsule walls without BHIM core material (Fig. 5.1 D).

5.1.1.2. *In vitro* release

BHIM was rapidly released, about 90% in 10 min at 23°C, from these microcapsules. Hence, any modification of these microcapsules was not attempted using this method.

5.1.2. PMMA Microcapsules by In-situ Polymerization

5.1.2.1. Size and shape analysis by SEM

A typical scanning electron micrograph taken from the resulting PMMA microcapsules is shown in Fig. 5.2. The microcapsules were spherical but the walls appeared to contain many pores, with the result that no BHIM solution could be effectively microencapsulated. Although their sizes were uniform and less than 10 μm, again no modification of these microcapsules was attempted using this method.

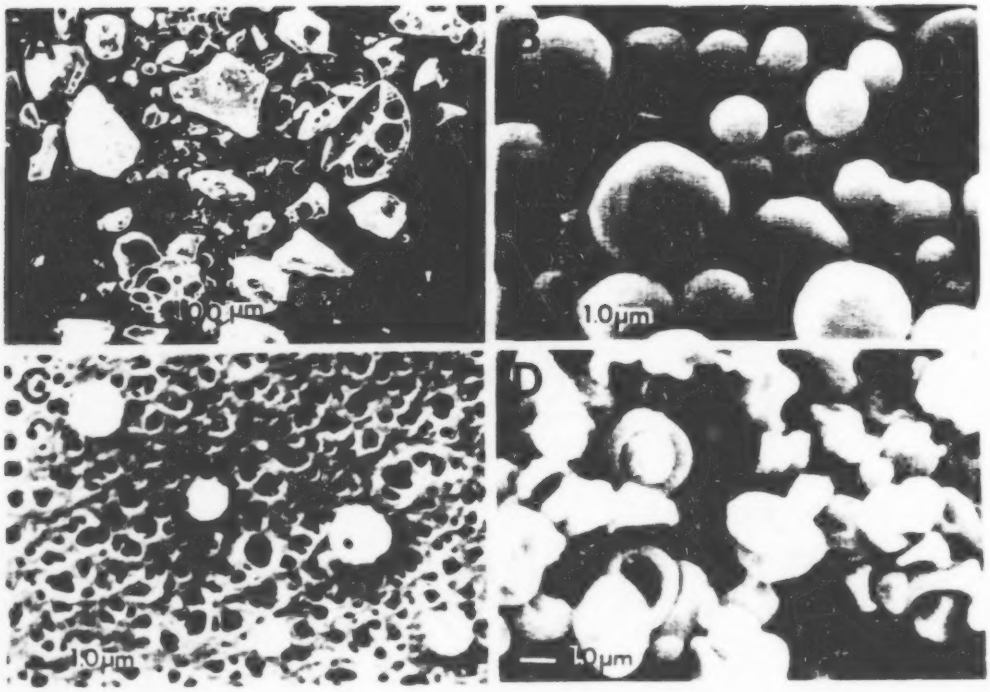
A
10.0 µm
B
1.0µm
C
1.0µm
D
1.0µm

Fig. 5.1 Scanning electron micrographs of BHIM powder and PMMA microcapsules: A. raw BHIM powder; B. spray-dried BHIM powder; C. 2.8% w/v PMMA microcapsules; D. 2.8% w/v PMMA blank microcapsules.

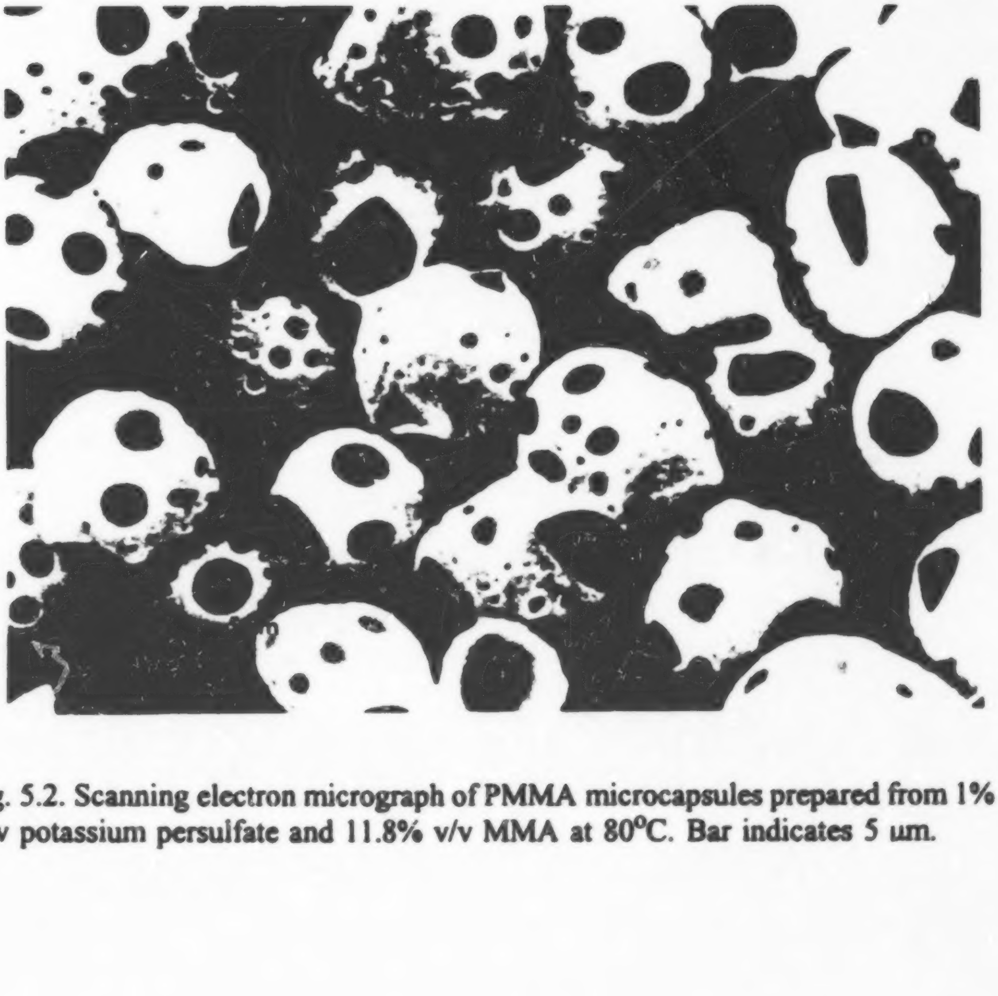

Fig. 5.2. Scanning electron micrograph of PMMA microcapsules prepared from 1% w/v potassium persulfate and 11.8% v/v MMA at 80°C. Bar indicates 5 um.

5.1.3. Polyamide Microcapsules by Interfacial Polymerization

5.1.3.1. Size and shape analysis by SEM

Polyamide microcapsules prepared from 20% w/v BHIM solution were characterized by SEM using a sample of microcapsules suspended in 50% w/v Tween 20 solution to prevent aggregation. A typical scanning electron micrograph of PPT microcapsules (Fig. 5.3) indicates spherical microcapsules of 1-4 μm in size.

5.1.3.2. BHIM loading, encapsulation efficiency and yield of microcapsules

The extent of BHIM loading of microcapsules was calculated using the following equation and the results are given in Table 5.1.

$$BHIM\ loading(\%) = \frac{BHIM_{encapsulated}(g)}{BHIM\text{-}loaded\ microcapsules(g)} x100 \qquad (5.1)$$

The results indicate that BHIM loading of PLT microcapsules was slightly higher than for PPT microcapsules at the two BHIM concentrations.

The yield of microcapsules was determined from:

$$Yield(\%) = \frac{BHIM\text{-}loaded\ microcapsules(g)}{Total\ input\ of\ incorporated\ agents(g)} x100 \qquad (5.2)$$

where the denominator includes the input amount of BHIM, sodium carbonate, water-soluble and water-insoluble monomers. The results are reported in Table 5.2. The yield was identical at 20% w/v BHIM concentration for each polyamide microcapsule but was apparently slightly greater for PPT microcapsules prepared

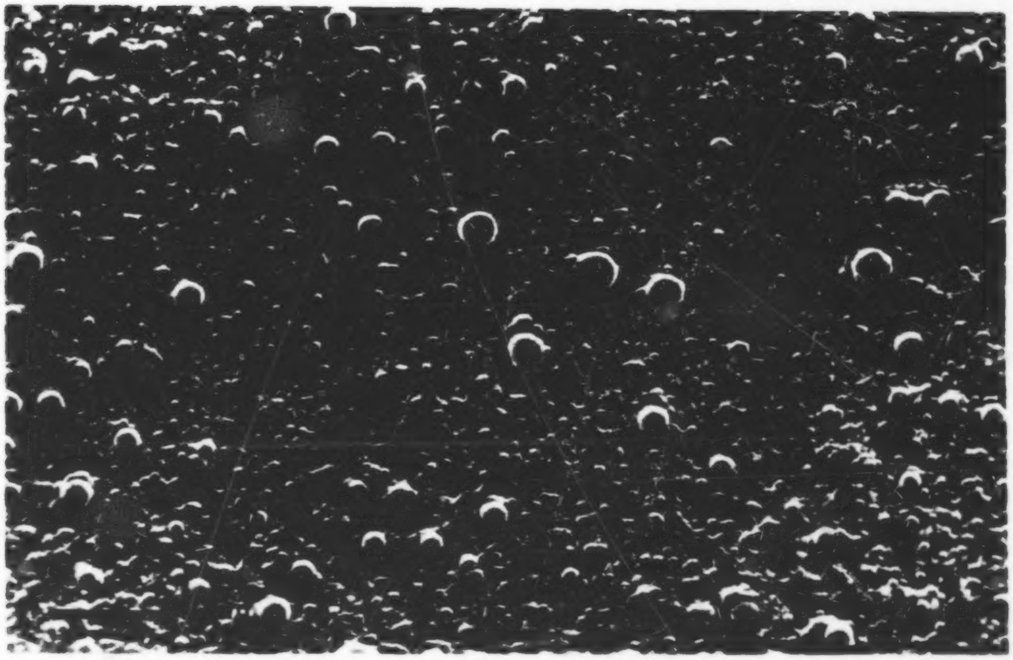

Fig. 5.3. Scanning electron micrograph of PPT microcapsules suspended in 50% Tween 20 solution. Bar indicates 10 μm.

Table 5.1. Loading of BHIM in polyamide microcapsules prepared at two BHIM concentrations.

BHIM concentration (% w/v)	BHIM loading (%) (mean±s.d.)[a]
PLT	
20	45.0±3.1
40	53.1±5.3
PPT	
20	34.5±4.4
40	22.0±0.9

[a] n=3 (batches).

Table 5.2. Yield of polyamide microcapsules prepared at two BHIM concentrations.

BHIM concentration (% w/v)	Yield (%) (mean±s.d.)[a]
PLT	
20	7.1±1.1
40	6.0±0.9
PPT	
20	7.8±0.7
40	10.2±0.7

[a] n=3 (batches).

from 40% w/v BHIM.

The encapsulation efficiency of BHIM (%), expressed as the fraction of the total BHIM which was encapsulated by the interfacial polymerization process, was calculated from,

$$\textit{Encapsulation efficiency}(\%) = \frac{\textit{Encapsulated BHIM}\ (g)}{\textit{BHIM added}\ (g)} x100 \qquad (5.3)$$

and the data are shown in Table 5.3. The encapsulation efficiency of PPT microcapsules was again apparently higher than in PLT microcapsules.

When the statistical t-test was applied to the above results, no significant difference in BHIM loading or yield of PLT microcapsules prepared at the two BHIM concentrations were found (Table 5.4). On the other hand, a significant difference was found in the encapsulation efficiency of BHIM. In contrast, applying the t-test to the results of the PPT microcapsules, significant differences in both BHIM loading and microcapsule yield were found, but no significant difference was found in encapsulation efficiency of BHIM.

5.1.3. *In Vitro* Release

Typical release profiles from PLT and PPT microcapsules are depicted in Fig. 5.4 and 5.5. Approximately 20-30% BHIM was released over a 5-day period, after which BHIM was released at a slower and almost constant rate for up to 40 days. However, the slower release period in some instances is characterized by an

Table 5.3. Encapsulation efficiency of BHIM in polyamide microcapsules prepared at two BHIM concentrations.

BHIM concentration (% w/v)	Encapsulation efficiency (%) (mean±s.d.)[a]
PLT	
20	4.2±0.3
40	3.3±0.3
PPT	
20	7.7±0.4
40	8.7±0.6

[a] n=3 (batches).

Table 5.4. Statistical analysis (t-test) of polyamide microcapsule formulation parameters at two BHIM concentrations (20% and 40% w/v).

Polyamide microcapsules	Formulation parameters	t-test value	t_4 at 2.5% l.s.	Difference*
PLT	% loading	2.29	2.78	NS
	% yield	1.30	2.78	NS
	% fraction	3.25	2.78	S
PPT	% loading	4.88	2.78	S
	% yield	4.24	2.78	S
	% fraction	2.41	2.78	NS

* significant (S) or no significant difference (NS).

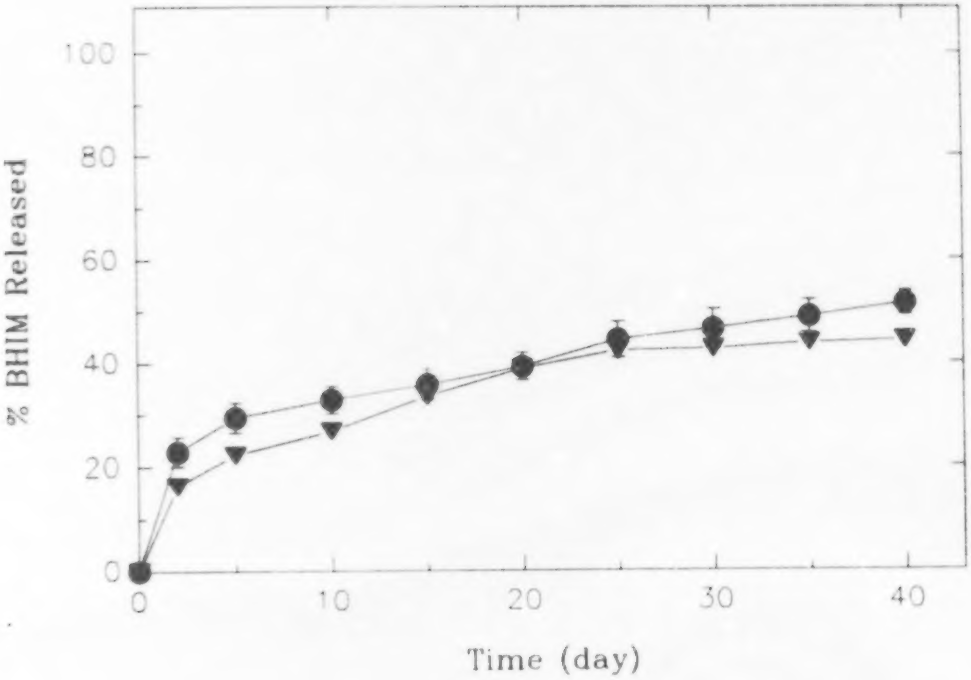

Fig. 5.4. The effect of BHIM concentration on the release of protein from PLT microcapsules at 23°C. (•) 20% w/v; (▾) 40% w/v. Values are the means of measurements from three different batches; the standard errors of the means are indicated. See Table 5.1 for corresponding loadings.

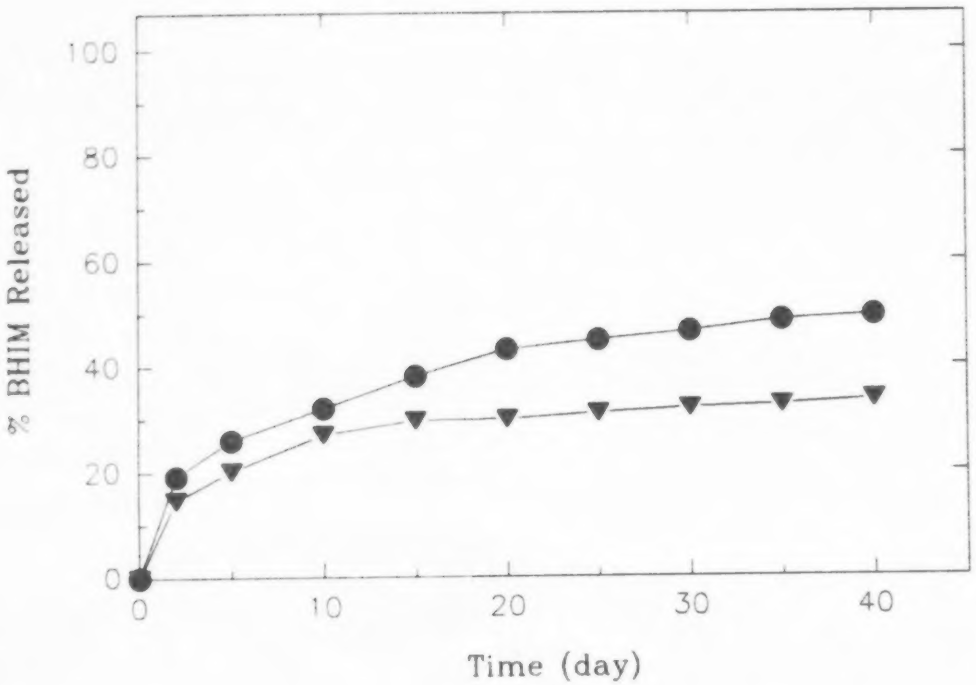

Fig. 5.5. The effect of BHIM concentration on the release of protein from PPT microcapsules at 23°C. (•) 20% w/v; (▾) 40% w/v. Values are the means of measurements from three different batches; the standard errors of the means fell within the symbol dimensions. See Table 5.1 for corresponding loadings.

apparent change to an even slower rate after about 20-25 days for PLT and PPT microcapsules prepared from 20% w/v BHIM concentration but after about 15 days for PPT microcapsules prepared from 40% w/v BHIM solution. Release rate constants determined from the different release periods are given in Table 5.5. There was a slight dependence of the release rate of protein from PPT but not PLT microcapsules.

The effect of temperature on the release profiles of protein from PLT and PPT microcapsules prepared with 20% w/v BHIM concentration are compared in Fig. 5.6 and 5.7, respectively. Increasing the temperature from 23°C to 40°C had a pronounced effect on the release rate of protein from both types of microcapsules. Almost 80 percent was released from PLT microcapsules at 40°C after 25 days compared to almost 100% from PPT microcapsules, more than double that released at 23°C from each of the two systems. It is interesting to observe, however, that the initial fast release from PLT microcapsules was shortened to 1 day with an increase in temperature followed by two slower release phases, a behaviour not observed with PPT microcapsules. A comparison of the release rate constants appears in Table 5.6. It can be seen that at 40°C, BHIM is released at the same rate from PLT and PPT microcapsules during the first slow release period whereas at 23°C BHIM is released faster from the PPT than from the PLT microcapsules

Table 5.5. Comparision of release rate constants (k) of BHIM from PLT and PPT microcapsules prepared at two BHIM concentrations at 23°C.

BHIM Conc. (% w/v)	k_1x10 (%day^{-1})	k_2x10 (%day^{-1})
PLT		
20	6.4±1.6[a]	---
40	10.8±1.4[a]	1.4±0.9[b]
PPT		
20	11.5±1.3[c]	3.3±0.7[b]
40	2.1±0.5[c]	---

[a] From day [5-25].
[b] From day [25-40].
[c] From day [5-12].

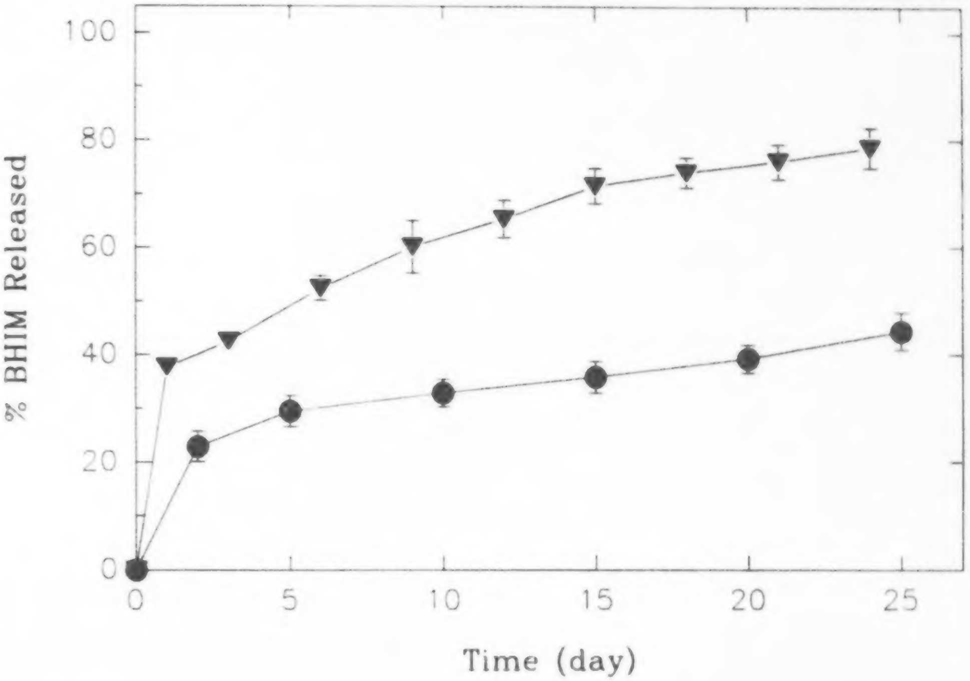

Fig. 5.6. The effect of temperature on the release of protein from PLT microcapsules prepared with 20% w/v BHIM solution, (•) 23°C; (▾) 40°C. Values are the means of measurements from three different batches; the standard errors from the means are indicated.

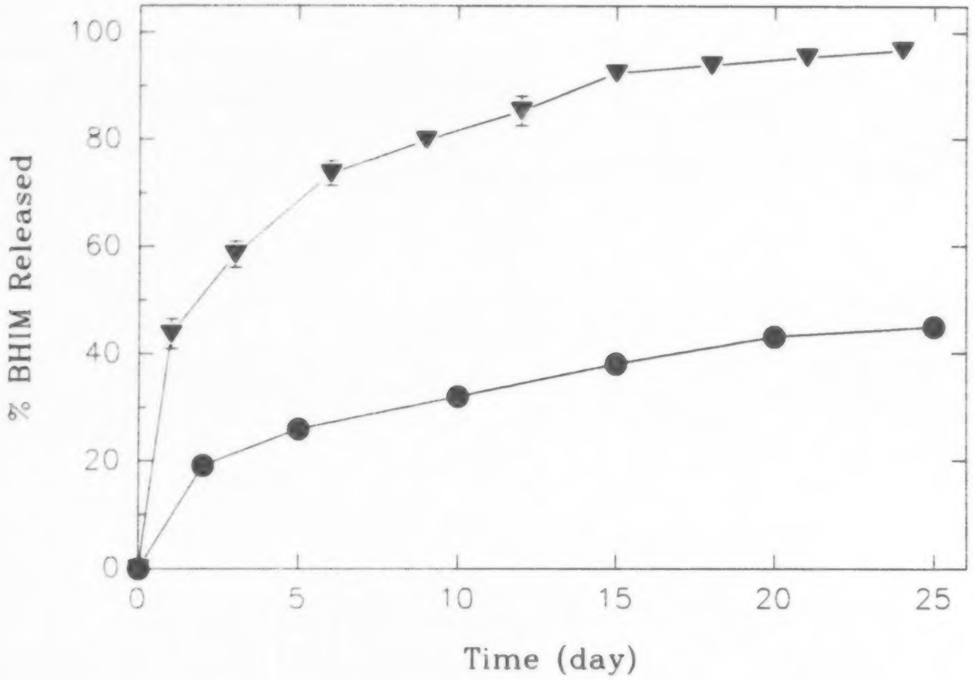

Fig. 5.7. The effect of temperature on the release of protein from PPT microcapsules prepared from 20% w/v BHIM solution, (•) 23°C; (▾) 40°C. Values are the means of measurements from three different batches, the standard errors from the means are indicated.

Table 5.6. Comparison of release rate constants (K) of BHIM from polyamide microcapsules prepared with 20% w/v BHIM at two temperatures.

Polyamide microcapsules	Temperature (°C)	K_1^ax10 (%day^{-1})	K_2^bx10 (%day^{-1})
PLT	23	6.4±1.6	---
	40	20.9±1.8	7.8±1.6
PPT	23	11.5±1.3	3.3±0.7
	40	20.6±3.7	4.9±0.7

[a] From day [6-15].
[b] From day [20-24].

during this period.

5.2. Microencapsulation of Dimenhydrinate

5.2.1. Process Evaluation of the Technique

5.2.1.1. Effect of stirring rate

Different batches of ethylcellulose microspheres at a polymer:drug 1:3 weight ratio were prepared at stirring rates of 200, 300, 400 and 500 rpm. At 200 rpm, no microspheres were formed. At 500 rpm, microspheres were smaller in size but nonspherical. The ideal stirring rates were either 300 or 400 rpm since these yielded microspheres which were spherical, discrete (unaggregated) and free flowing as a powder. A typical microsphere prepared at 300 rpm can be seen from a SEM micrograph in Fig. 5.8 A. The surface of the microsphere was not smooth or uniform but had a sponge-like appearance which seemed to be an agglomeration of elongated polymer strands (Fig. 5.8 B) in which drug was embedded.

The results of size analysis of batches of various microspheres are summarized in Table 5.7, Fig. 5.9 and 5.10. At a preparation stir rate of 400 rpm, the mean size of the microspheres was smaller (380 μm) than at 300 rpm (480 μm) and a log-normal distribution of sizes is evident, although the distribution is somewhat skewed and unsymmetric for microspheres prepared at 400 rpm (Fig. 5.9) and this is confirmed in Fig. 5.10 (i.e. linearity of the log-probability plots of size versus cumulative percent under size).

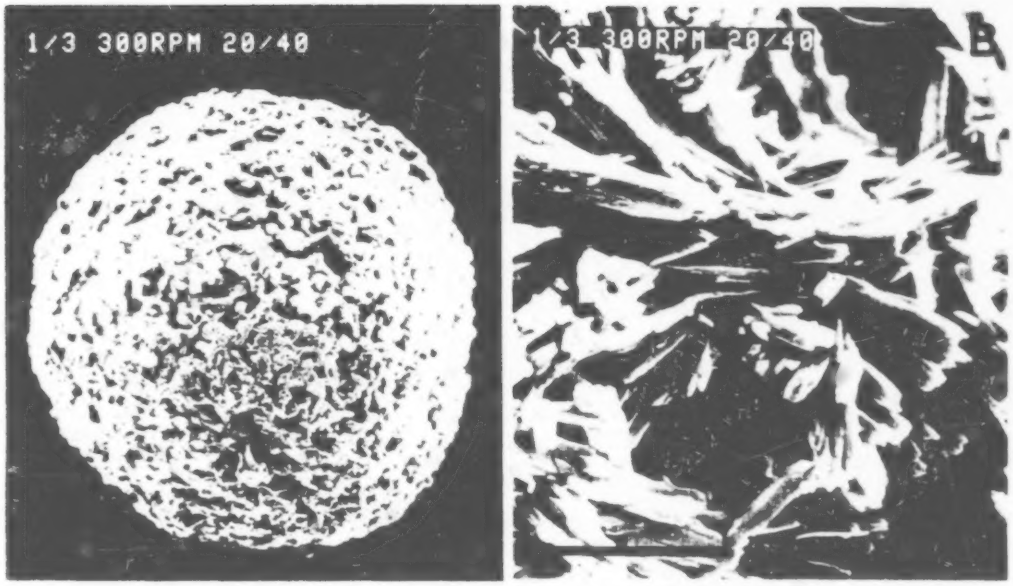

Fig. 5.8. Scanning electron micrographs of ethylcellulose microspheres of dimenhydrinate 1:3 polymer:drug sieve size fraction 20/40 prepared at 300 rpm. A. Spherical ethylcellulose microsphere. Bar indicates 100 μm. B. Surface morphology of microsphere. Bar indicates 10 μm.

Table 5.7. Size analysis of ethylcellulose microspheres of dimenhydrinate (1:3 polymer:drug ratio).

Sieve number (passed/ retained)	Size range (µm)	Percentage retained		Percentage less than maximum of the stated size	
		Stirring rates		Stirring rates	
		300 (rpm)	400 (rpm)	300 (rpm)	400 (rpm)
60/120	125-250	---	3.04	---	3.04
50/60	250-297	0.27	9.66	0.27	12.7
40/50	297-425	14.5	58.1	14.7	70.8
30/40	425-600	79.3	26.3	94.0	97.1
20/30	600-841	6.01	2.89	100	100
Geometric mean size[a] (diameter) (µm):				480	380
Geometric standard deviation[b] (σ)				1.19	1.32

---

[a] size corresponding to 50% value on the probability scale.

[b] $= \frac{\text{84\% undersize}}{\text{50\% size}}$ on the probability scale.

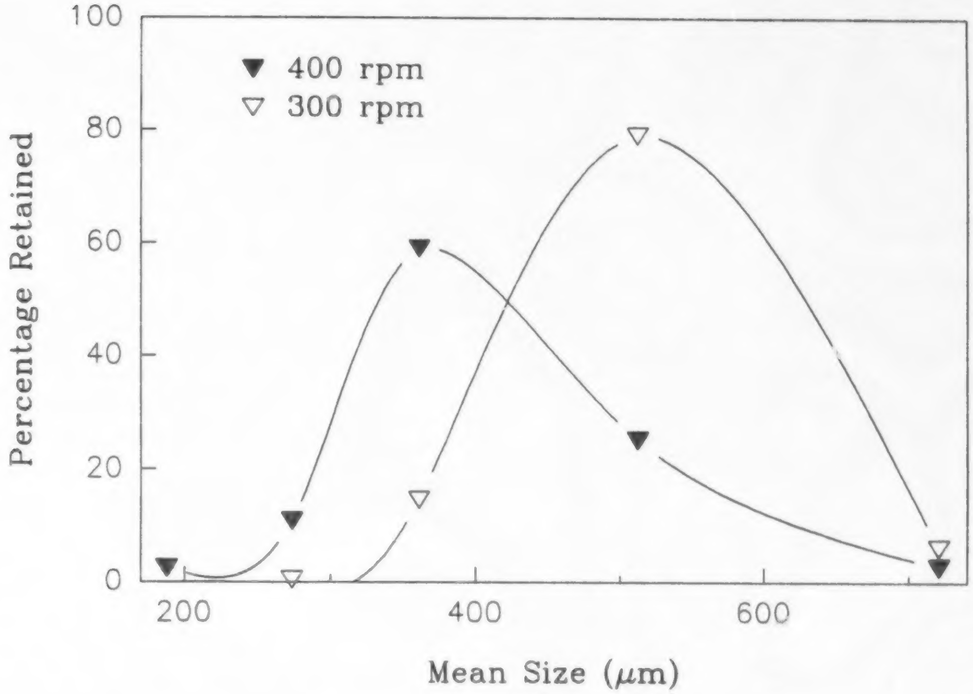

Fig. 5.9. Size distribution of ethylcellulose microspheres of dimenhydrinate (1:3 polymer:drug) prepared at two stirring rates.

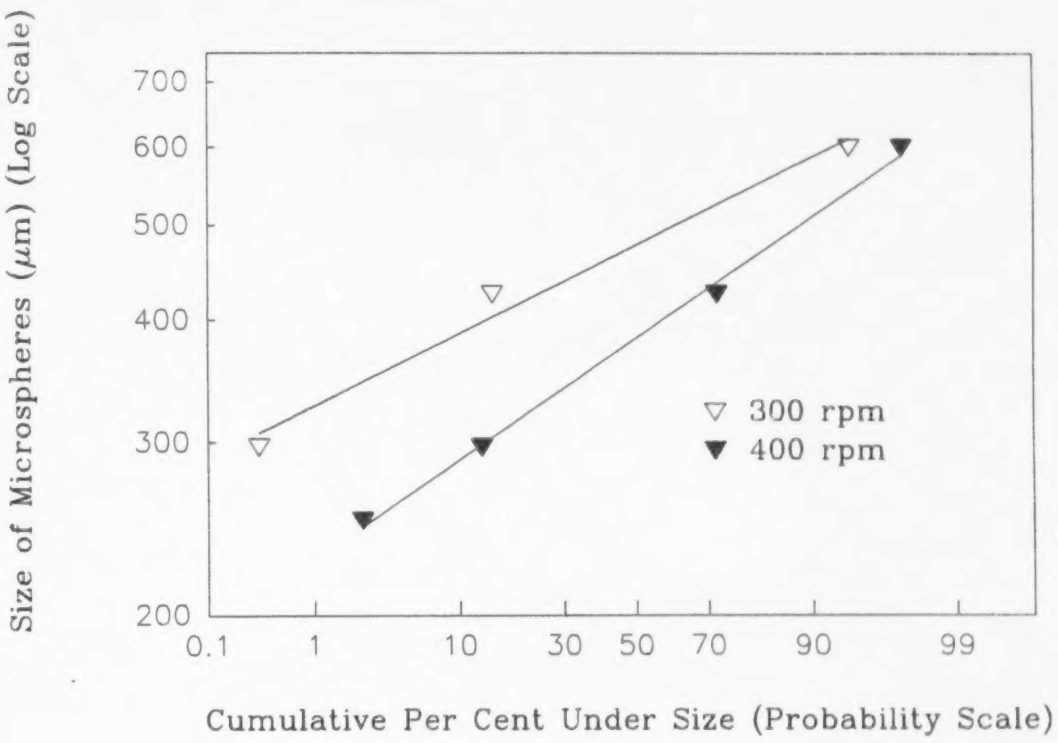

Fig. 5.10. Log-probability plots for size distribution of ethylcellulose microspheres of dimenhydrinate (1:3 polymer:drug) prepared at two stirring rates.

5.2.1.2. Influence of surfactant

Two batches of microspheres at polymer:drug 1:3 weight ratio were prepared at 400 rpm, one containing 1% w/v Span 80 and one containing no Span 80 (i.e. only mechanical emulsification). The surfactant was included in a mixture of light mineral oil and heptane prior to emulsification.

In the absence of Span 80, a uniform emulsion was formed by mechanical stirring, however, the dispersed phase globules aggregated (see Experimental) while the solvent was being slowly evaporated. This resulted in no microspheres being formed under these conditions. On the other hand, when Span 80 was included as emulsifying agent, spherical microspheres were obtained.

5.2.2. Test of Reproducibility of the Method

Three batches of polymer:drug, 1:3 weight ratio microspheres were prepared at 300 rpm and the reproducibility of the technique was assessed on the basis of size distribution of the microspheres produced and uniformity of drug content.

5.2.2.1. Particle size distribution

The various size ranges of a batch of microspheres were separated by sieving using a range of standard sieves and the amounts retained on the sieves were weighed. The weight percentage of each sieve size fraction and the cumulative per cent less than maximum of the stated size are summarized in Table 5.8. The size distributions of microspheres (Fig. 5.11), the linearities of the size distribution data represented as log-probability plots of diameter versus cumulative percent under size (Fig. 5.12) and the geometric mean diameters of 480 µm all illustrate the close agreement of the results for each batch.

5.2.2.2. Drug content of microspheres

The loading of dimenhydrinate in microspheres was determined for three batches of sieve size fraction 20/40. The means, standard deviations (s.d.) and C.V. were calculated from,

$$Mean(x)=\frac{\sum x}{n} \qquad (5.4)$$

$$Standard\ deviation(s)=\frac{n\sum x^2-(\sum x)^2}{n(n-1)} \qquad (5.5)$$

$$C.V.=\frac{s.d.}{mean}x100 \qquad (5.6)$$

where x represents the variable parameter (i.e., individual observation) and n is the number of observations.

The results, given in Table 5.9, indicate reproducibility of the mean percent dimenhydrinate contents (69.65±0.52, 68.96±0.62 and 70.49±0.57, respectively). Further statistical analysis is given in Table 5.10. The coefficient of variation (C.V.) was 1.10% and the analysis of variance indicate that the percent drug content was not significantly different for the three batches of microspheres.

Table 5.8. Size analysis of different batches of ethylcellulose microspheres of dimenhydrinate (1:3 polymer:drug) prepared at 300 rpm.

Sieve number (passed/ retained)	Size range (µm)	Percentage retained			Percentage less than maximum of the stated size		
		Batch I	Batch II	Batch III	Batch I	Batch II	Batch III
50/60	250-297	0.27	0.42	0.27	0.27	0.42	0.27
40/50	297-425	14.5	14.9	14.5	14.8	15.3	14.8
30/40	425-600	79.3	78.5	79.5	94.1	93.8	94.3
20/30	600-841	6.01	6.32	5.83	100	100	100
Geometric mean size[a] (diameter) (µm):					480	480	480
Geometric standard deviation[b] (σ)					1.19	1.19	1.19

[a] size corresponding to 50% value on the probability scale.

[b] $\frac{\text{84\% undersize}}{\text{50\% size}}$ on the probability scale.

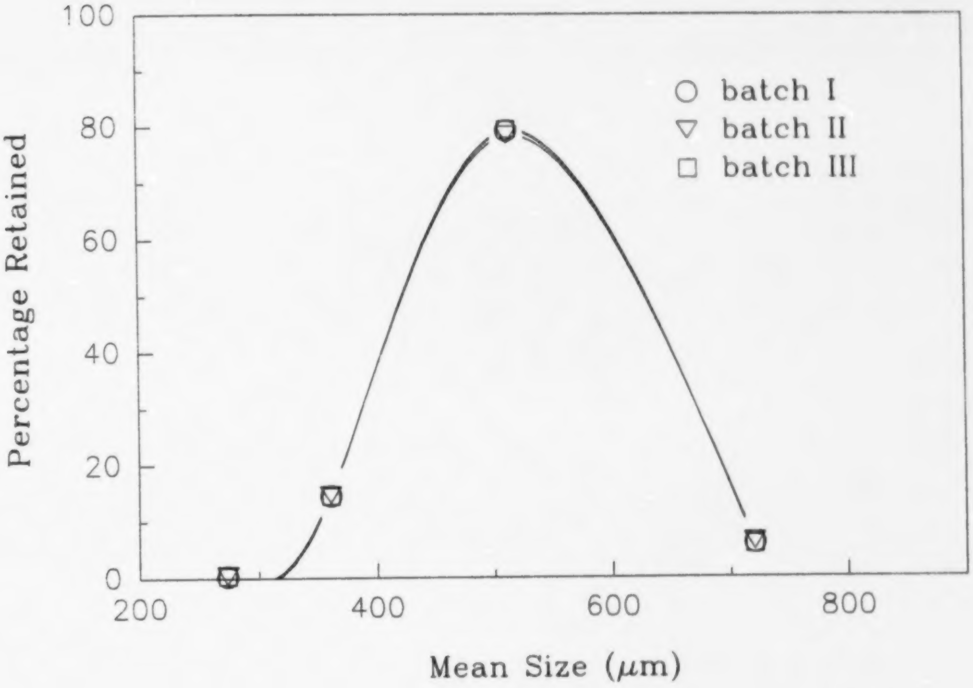

Fig. 5.11. Size distribution of three batches of ethylcellulose microspheres of dimenhydrinate prepared at 300 rpm.

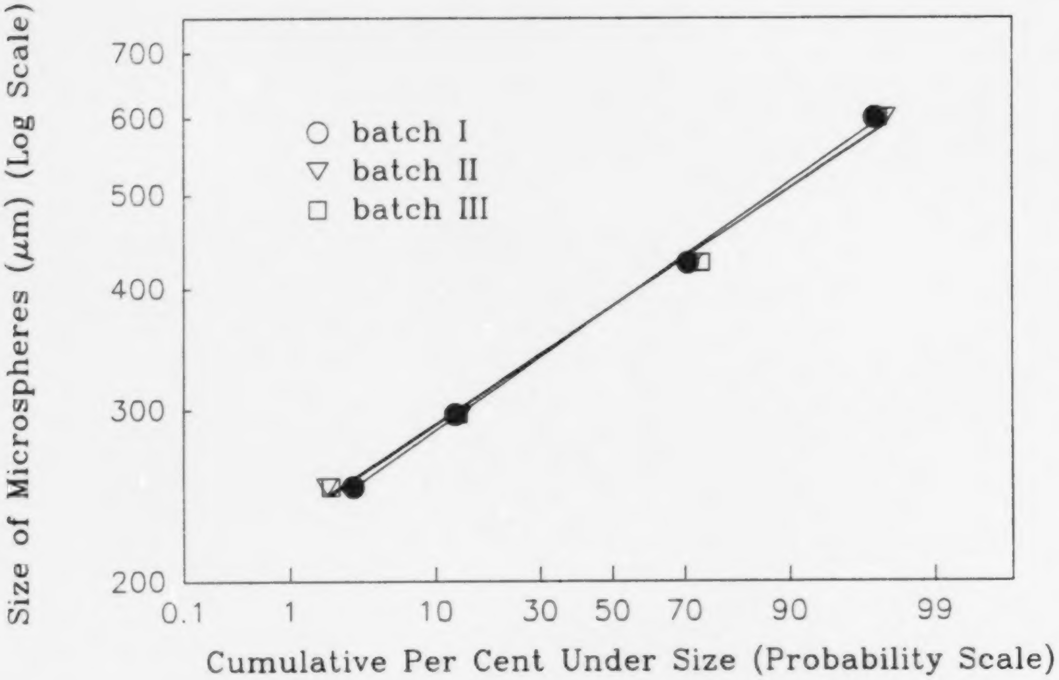

Fig. 5.12. Log-probability plots of the size distribution of three batches of ethylcellulose microspheres prepared at 300 rpm.

Table 5.9. Dimenhydrinate content of ethylcellulose 20/40 sieve size microspheres (1:3 polymer:drug) prepared at 300 rpm.

Batch number	Percent dimenhydrinate content in sample			Mean percent dimehydrinate content ± s.d.
	1	2	3	
I	69.5	69.2	70.2	69.7±0.52
II	68.4	68.9	69.6	69.0±0.62
III	69.9	70.5	71.1	70.5±0.57
Average				69.7±0.77
C.V.= 1.10%				

Table 5.10. Analysis of variance of results in Table 5.9.

Null hypothesis (H_o): There was no significant difference between the percent dimenhydrinate contents in the microspheres of different batches prepared under similar conditions.

Source of variation	Degrees of freedom	Sum of squares	Mean sum of squares	F	$F_{(v,u)}$
Batch	2	3.52	1.76		$F_{(2,6)}$ at
Error	6	1.95	0.33	5.33	2.5%= 7.26
Total	8	5.48			

Result: H_o is acceptable since the calculated value of the F ratio is less than the Table $F_{2,6}$ at 2.5% level of significance. Thus, there was no significant difference in the dimenhydrinate content of microspheres from three batches prepared under similar conditions.

5.2.3. Microspheres at Various Polymer:Drug Ratios

Microspheres were prepared as described earlier at 300 or 400 rpm at ethylcellulose:dimenhydrinate weight ratios of 1:1, 1:3 and 1:5.

5.2.3.1. Particle size distribution

The size distribution of microspheres at all polymer to drug ratios was confirmed as being log-normal (Fig. 5.13). The geometric mean sizes at 1:3 and 1:5 polymer:drug ratios prepared at 300 rpm were 480 and 700 μm, respectively. However, at 1:1 polymer:drug ratio, no dimenhydrinate was microencapsulated. At 400 rpm, the geometric mean sizes of the 1:1, 1:3 and 1:5 polymer:drug ratios were 280, 380 and 460 μm, respectively. Thus, as the amount of drug increased, the mean size of microspheres also increased. Also, Fig. 5.14 shows the size distributions of the microspheres prepared at the two stirring rates, i.e. the higher the stirring rate, the smaller the particles. The size distributions were unimodal except for microspheres prepared at 400 rpm at 1:1 polymer:drug ratio, which exhibited a bimodal distribution, indicating that the aggregation of particles played a significant role during their formation.

5.2.3.2. Efficiency of drug loading

Table 5.11 compares the drug content of various dimenhydrinate ethylcellulose microsphere formulations as a function of the sieve size fraction, the

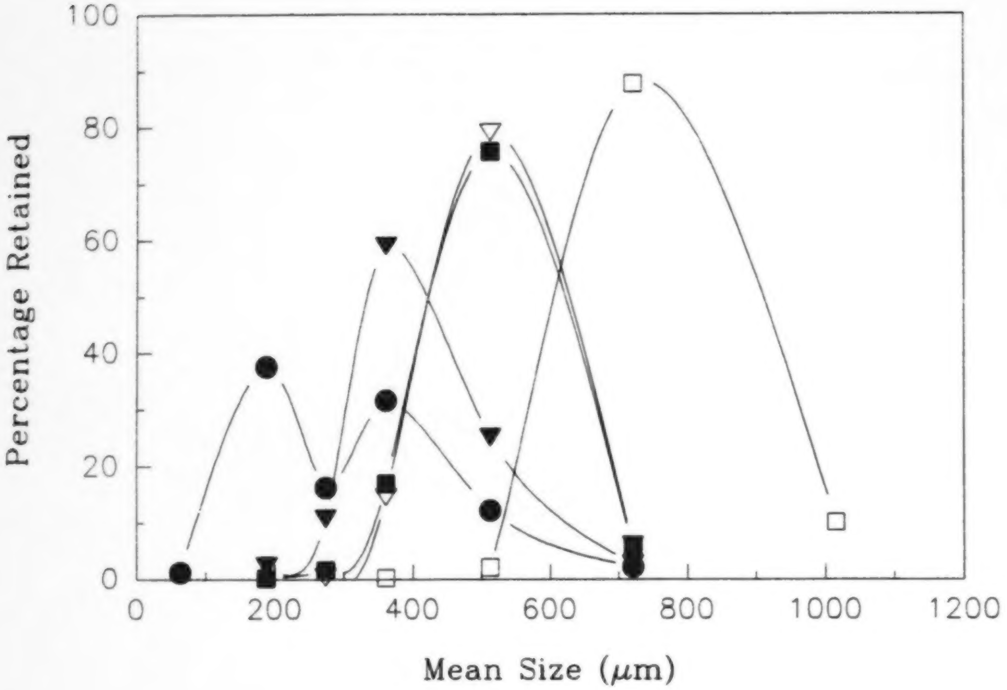

Fig. 5.13. Size distribution of ethylcellulose microspheres of dimenhydrinate at various drug loadings prepared at two stirring rates. 300 rpm (open symbols); 400 rpm (closed symbols). (•), 1:1, polymer:drug; (▿, ▾), 1:3, polymer:drug; (▫, ▪), 1:5, polymer:drug. Data points represent the means of measurements in three different experiments; the standard errors of the means fell within the symbol dimensions.

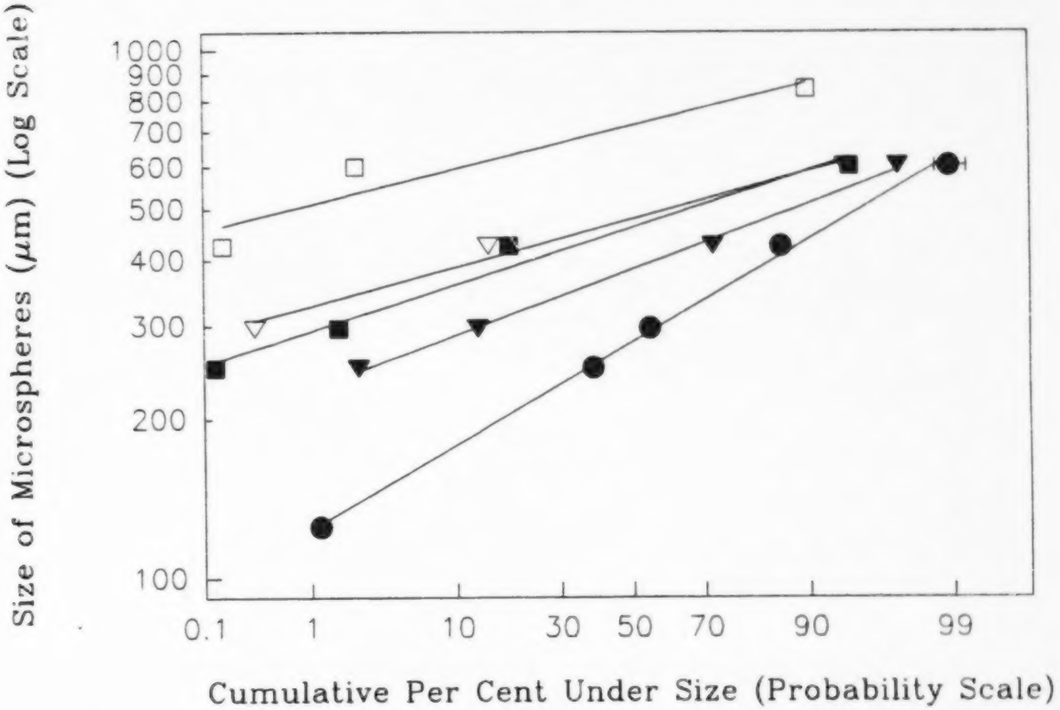

Fig. 5.14. Log-probability plots of the size distributions of ethylcellulose microspheres at various drug loadings prepared at two stirring rates, 300 rpm (open symbols); 400 rpm (closed symbols). (•), 1:1, polymer:drug; (▿, ▾), 1:3, polymer:drug; (▫, ▪), 1:5, polymer:drug.

Table 5.11. Comparison of the drug content of two sieve size fractions of dimenhydrinate ethylcellulose microsphere formulations at three drug loadings.

Polymer/drug	Stirring rate(rpm)	Mean percent drug content (± s.d.)		t-test value	t_4[a] at 2.5% l.s.	Difference[b]
		20/40	40/60			
1/3	300	69.3±0.80	40.4±2.83	17.0	2.78	S
1/5		83.9±1.90	95.9±2.41	6.79	2.78	S
1/1	400	20.6±1.36	27.2±0.90	6.96	2.78	S
1/3		73.6±5.31	79.3±4.11	1.46	2.78	NS
1/5		89.2±0.45	95.8±1.62	6.80	2.78	S

[a] t value at degree of freedom = $n_1 + n_2 - 2 = 4$, n is the number of batches.
[b] significant (S) or no significant (NS) difference at 2.5% level of significance.

stirring rate during preparation, and the polymer:drug ratio. Thus, in each case at the same polymer:drug ratio and the 20/40 sieve size fraction of microspheres the drug content of the microspheres increased slightly when the stirring rate during preparation increased from 300 rpm to 400 rpm. In contrast, at 1:3 polymer:drug ratio the drug content of the 40/60 sieve size fraction of microspheres doubled when the stirring rate was increased from 300 to 400 rpm. However, the drug content was identical and almost 100 percent of the weight of microspheres at the 1:5 polymer:drug ratio when compared under the same conditions. As expected, the drug content increased in all cases where the initial amount of drug in the system increased. Statistically, the differences in drug content observed between the two sieve size fractions were significant for all polymer:drug ratios except for the 1:3 polymer:drug ratio microspheres prepared at 400 rpm.

5.2.4. Drug Release Studies

The release profiles of dimenhydrinate obtained from the 20/40 and 40/60 sieve size fractions of microspheres at the various polymer:drug ratios are depicted in Fig. 5.15 at the 300 rpm and Fig. 5.16 at the 400 rpm preparation stir rates. Generally, the release is characterized by an initial fast release extending from about 60 min to 120 min then a slower release phase. At a stirring rate of 300 rpm during preparation, the smaller the microspheres and the greater the drug loading, the faster was the rate of release. The effect of drug loading on release was more pronounced from the smaller microspheres. At a stirring rate of 400 rpm during

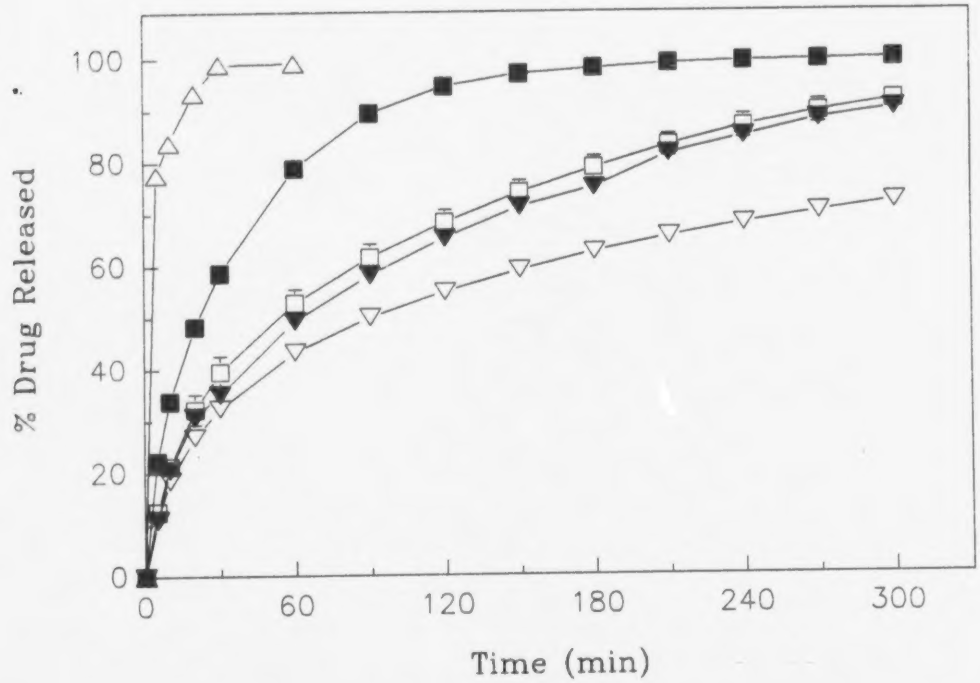

Fig. 5.15. Release of dimenhydrinate from ethylcellulose microspheres prepared at 300 rpm in water at 37°C for two different sieve size ranges, 250-425 μm (closed symbols), 425-841μm (open symbols). (▼, ▽), 1:3, polymer:drug; (■, □), 1:5, polymer:drug. The dissolution of dimenhydrinate powder (△), is shown for comparison. Values are the means of measurements from three different experiments; bars indicate the standard errors of the means.

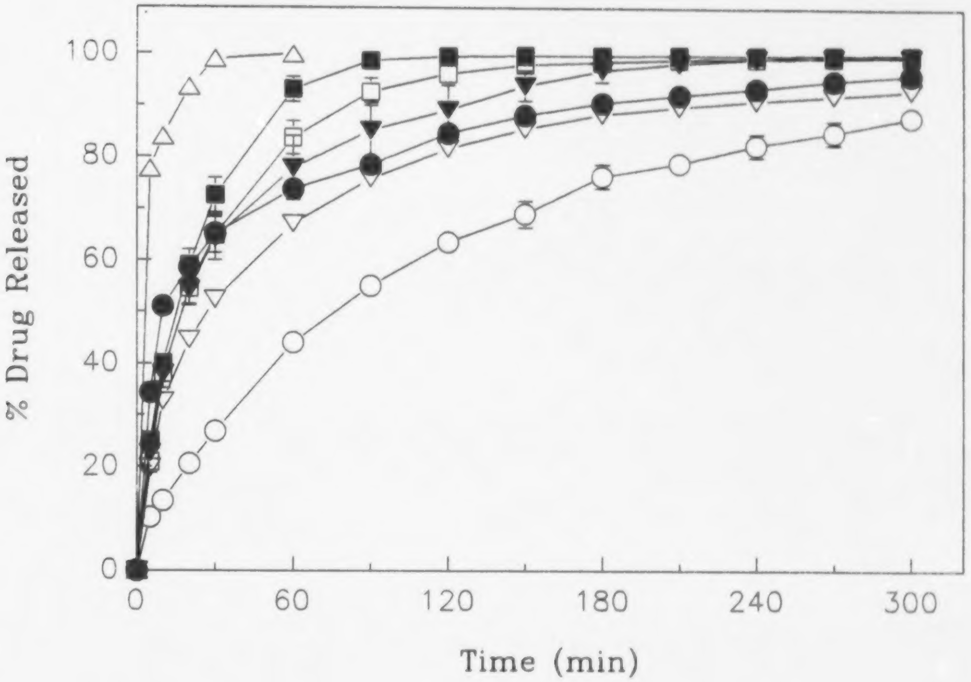

Fig. 5.16. Release of dimenhydrinate from ethylcellulose microspheres prepared at 400 rpm in water at 37°C for two different sieve size ranges, 250-425 μm (closed symbols), 425-841μm (open symbols). (○), 1:1, polymer:drug; (▼, ▽), 1:3, polymer:drug; (■, □), 1:5, polymer:drug. The dissolution of dimenhydrinate powder (△), is shown for comparison. Values are the means of measurements from three different experiments, bars indicate the standard errors of the means.

preparation, the effect of drug loading was most pronounced for the larger microspheres when the composition was 1:1 polymer:drug. In all cases, the availability of dimenhydrinate to the dissolution medium from microspheres was markedly less than from the drug powder at any given time and release was sustained for time periods ranging from 1 to at least 10 h depending on the particle size and drug loading (cf. ~30 min dissolution time of the powdered drug).

Reproducibility of the release behaviour from 3 different batches of microspheres is shown in Table 5.12 for 20/40 and 40/60 sieve size fractions, respectively. The time taken for 50% of the dimenhydrinate to be released ranged from 78 to 17 min for the larger size 20/40 sieve size microspheres and from 63 to 10 min for the smaller 40/60 sieve size microspheres. Variation among the batches was less than 25 percent of the mean. A plot of the T_{50} against the wt.% of ethylcellulose using the 20/40 sieve size fraction of microspheres prepared at a stirring rate of 400 rpm was linear as shown in Fig. 5.17 (r = 0.998).

5.3. Microencapsulation of Diphenhydramine HCL

In an attempt to prepare sustained release microcapsules of this very water-soluble salt form of the drug (1 g/ml), a hydrophobic polymer was selected. Two widely employed hydrophobic polymers in microencapsulation are ethylcellulose and Eudragit RS 100 and processes used to prepare microcapsules with these polymers are well-known. In my hands, microcapsules could be prepared in each

Table 5.12. Comparison of the T_{50} of dimenhydrinate from two sieve size fractions of ethylcellulose microspheres prepared at three drug loadings.

Stirring rates (rpm)	Polymer/Drug	T_{50}[a] (min)	
		20/40	40/60
300	1/3	77.7±14.3	62.7±3.8
	1/5	51.0±12.2	20.7±0.8
400	1/1	78.1±7.7	9.57±0.4
	1/3	27.4±1.7	17.4±3.0
	1/5	17.2±3.1	15.0±2.2

[a] Time (min) for 50% of drug to be released from microspheres; values are the means±s.d. for three batches of samples prepared under similar conditions.

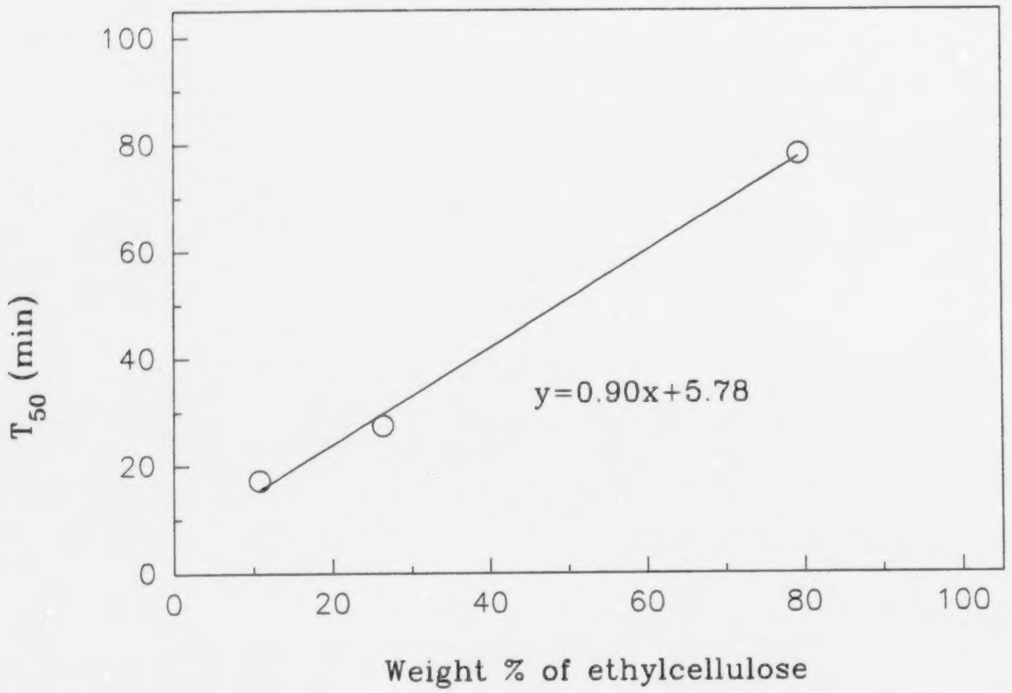

Fig. 5.17. Dependence of the time for 50 percent dimenhydrinate to be released (T_{50}) from 20/40 sieve size fraction ethylcellulose microspheres prepared at 400 rpm as a function of weight percentage of coating material (correlation coefficient = 0.998). Values are the means of measurements from three different experiments; the standard errors of the means fell within the symbol dimensions.

instance but, unfortunately, the microcapsule walls did not provide much of a barrier to drug diffusion. Only results using Eudragit RS 100 to make microcapsules are reported here.

5.3.1. Examination of Microcapsules by OM and SEM

Microcapsules prepared from 8% w/v Eudragit RS 100 in the presence of 6% w/v PIB as an anti-aggregating agent were observed by optical microscope (OM). The photomicrograph of a typical microcapsule, as shown in Fig. 5.18, indicates a drug particle coated within a polymeric membrane. A scanning electron micrograph of a dried microcapsule is shown in Fig. 5.19. provides evidence that the surface of the Eudragit RS 100 coating possesses numerous defects which could be the source of leakage of entrapped drug once dissolved in the aqueous medium.

5.3.2. Effect of Eudragit RS 100 Concentration on *In Vitro* Release

The effect of different concentrations of Eudragit RS 100 (4, 8 and 12% w/v) on the release of diphenhydramine HCl at a fixed 4:1 ratio of polymer:drug was examined. PIB was included as an anti-aggregating agent at a 6% w/v concentration. Diphenhydramine HCl microcapsules were sieved before the release studies and the 250-425 μm sieve-size fraction was selected. Release studies were carried out in pH 7.4 phosphate buffer at 37°C. The results shown in Fig. 5.20 clearly indicate that the microcapsules offered little improvement in the availability of drug to the aqueous medium compared to the powdered drug.

5.3.3. Effect of PIB Concentration

The possible influence of the inclusion of PIB on the properties of the microcapsules was also examined and the results on release of diphenhydramine HCL are shown in Fig. 5.21. The effect was minimal but at 6% w/v, PIB appeared to cause a decrease in the release rate which was the reason for using this concentration in the other studies.

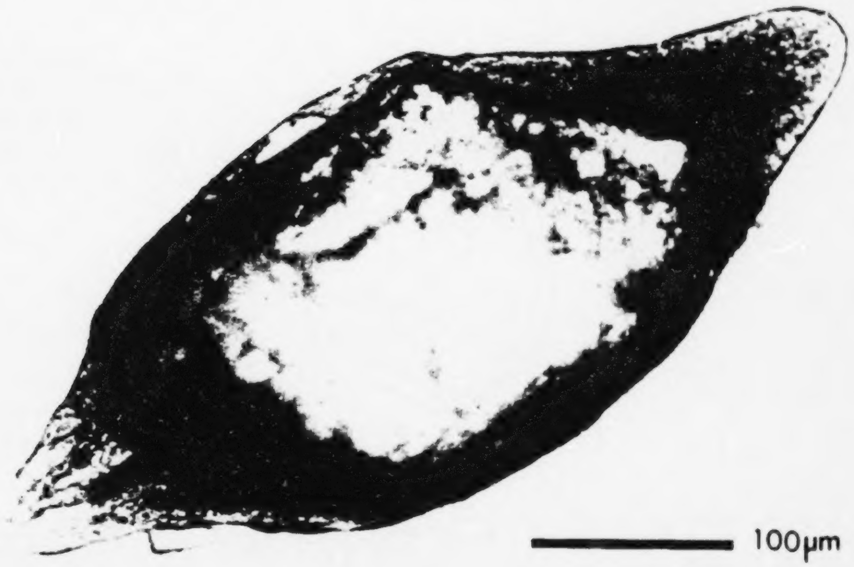

Fig. 5.18. Optical micrograph of 8% w/v Eudragit RS 100 microcapsule. Bar indicates 100 µm.

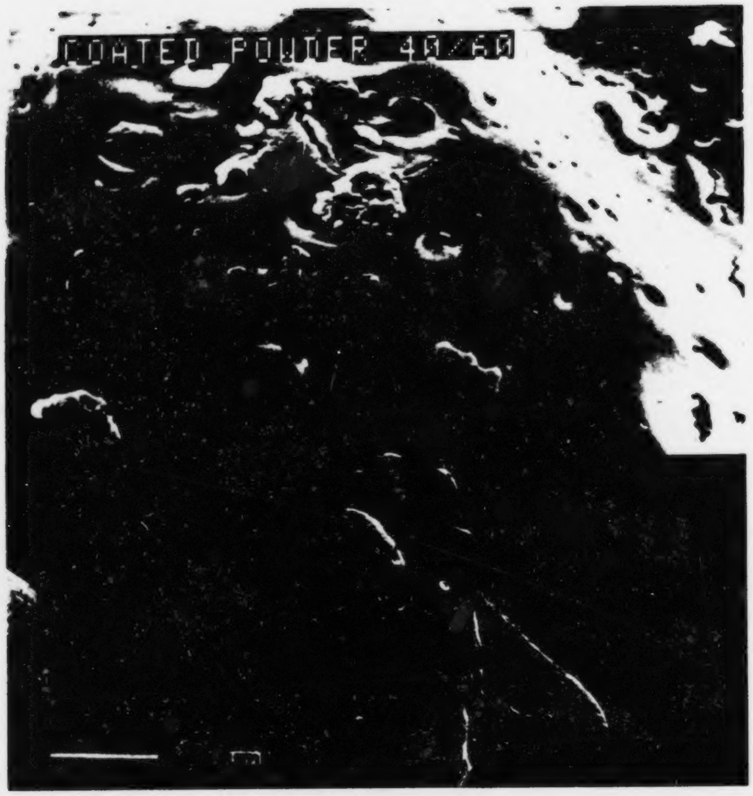
COATED POWDER 40/60

Fig. 5.19. Scanning electron micrograph of 8% w/v Eudragit microcapsule of sieve size fraction 40/60. Bar indicates 100 μm.

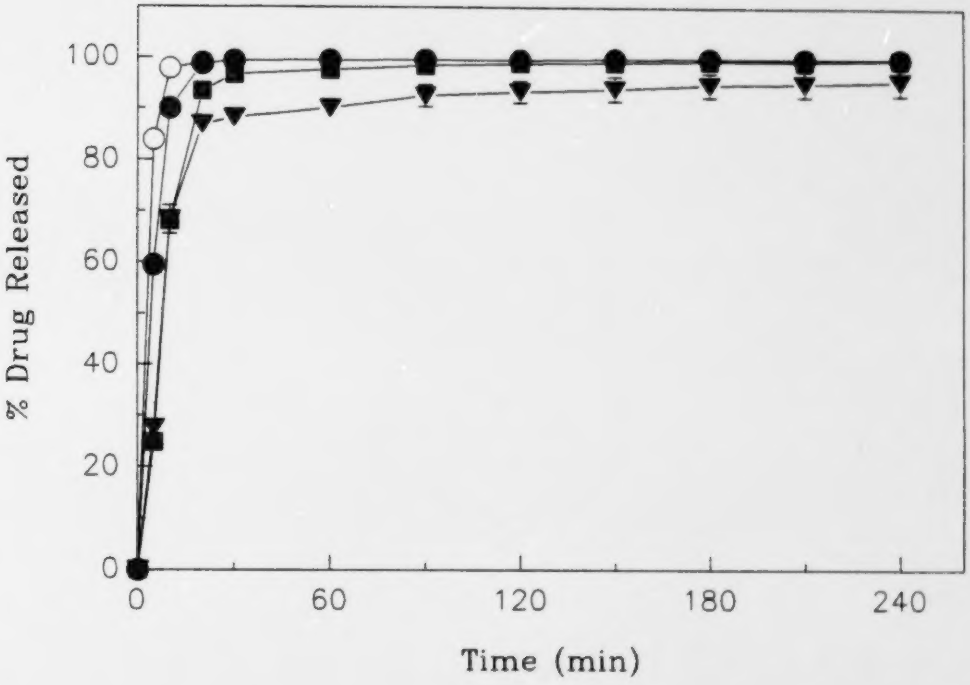

Fig. 5.20. Release of diphenhydramine HCl in pH 7.4 phosphate buffer at 37°C from 40/60 sieve size microcapsules as a function of Eudragit RS 100 concentration, (•), 4% w/v; (▾), 8% w/v; (▪), 12% w/v. PIB concentration was fixed at 6% w/v. Values are the means of measurements from three different batches, bars indicate the standard error of the means. The dissolution of diphenhydramine HCl is shown for comparison (○).

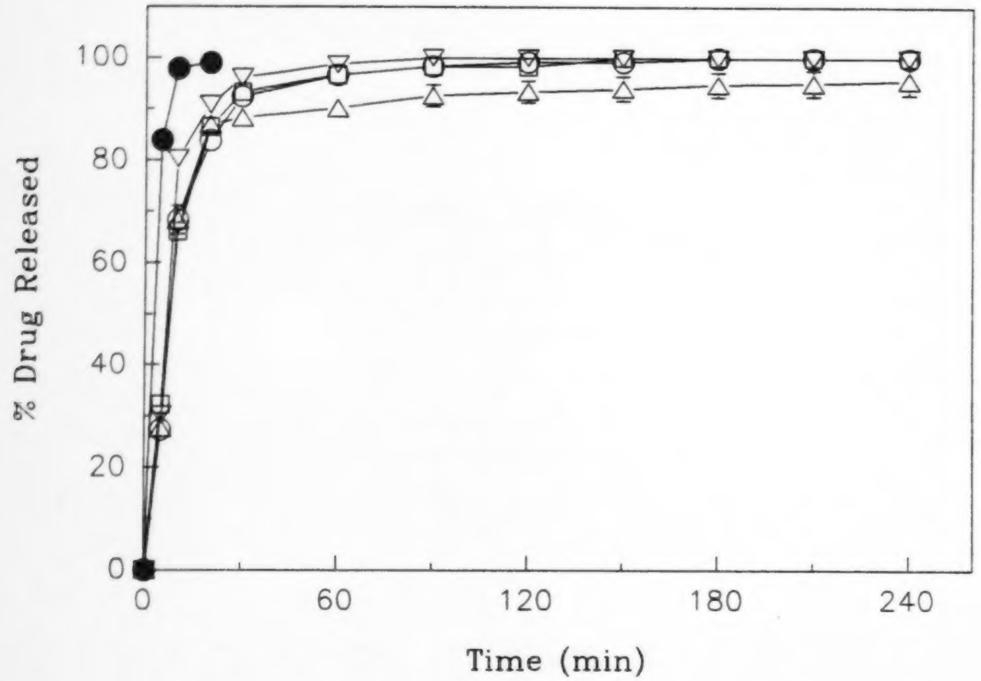

Fig. 5.21. Release of diphenhydramine HCl from 8% w/v Eudragit RS 100 microcapsules of sieve size 40/60 as a function of concentration of PIB. (▫), 3% w/v; (▿) 4% w/v; (◦) 5% w/v; (▵), 6% w/v. Values are the means of measurements from three different batches, bars indicate the standard error of the means. The dissolution of diphenhydramine HCl is shown for comparison (◦).

CHAPTER VI

6. DISCUSSION

6.1. BHIM

There are several techniques for preparing polymeric microcapsules, as was previously mentioned. Each technique is dependent on the type of polymer to be employed and the specific set of objectives to be met. In the case of microencapsulation of the water-soluble heterogeneous nutrient, BHIM, for co-injection with UMBs in a high permeability zone of an oil reservoir, the specifications of the final product were somewhat challenging. It was necessary to achieve a reasonable encapsulation efficiency, a microcapsule size of less than 1 µm, robustness of the microcapsules during injection, a SR of BHIM for approximately 30 days with delayed release for at least 24 hr, all of which could be produced with a yield that would not cause the costs of processing to be exorbitant.

Using PMMA as a polymeric material, which has been widely employed successfully to microencapsulate hydrophobic (lipophilic) materials, to formulate water-soluble materials was not very successful. Although it was believed that microcapsules having hydrophobic walls would provide a relatively slow release of a water-soluble substance, this was not the case.

As the SEM micrograph (Fig. 5.1 C) indicates a single pinhole occurred on each microcapsule. Consequently, the BHIM inside the microcapsules was rapidly dissolved by the infusing aqueous medium and the solution was rapidly released.

The principle of microcapsule formation by spray drying involves rapid solvent evaporation and deposition of polymer on adjacent particle surfaces. Furthermore, it is likely that very small particles of BHIM could become trapped in the polymer matrix during the drying process. The rate of evaporation of solvent, and the ratio of polymer to core material determine the extent to which this might occur. The smallest particle size achieved was about 1 μm, which was near the desired size.

Likewise, BHIM microcapsules prepared by in-situ polymerization using MMA did not provide the sustained release of BHIM which was anticipated. Again, the SEM micrograph (Fig. 5.2) clearly shows microcapsules with large pores in their surfaces, more than those prepared by spray drying. Consequently, most of the BHIM within or on the surface was removed during the solvent washing step in the process.

In in-situ polymerization, thermal scission and redox reaction brought about free radical polymerization, using potassium persulfate as the water-soluble initiator. It is important to consider the means of initiation since it can be shown by Eq.(6.1) that the instantaneous rate of polymerization at steady-state depends directly on the square root of rate initiation.

$$\frac{-d[M]}{dt}=\frac{k_p[M]^{1/2}}{k_t^{1/2}}(\textit{rate of formation of monomer-ended radicals})^{1/2} \qquad (6.1)$$

[M] is the monomer concentration, k_p is the propagation rate constant and k_t is the overall termination constant. Factors, such as concentration of the initiator, the presence of ferrous sulfate, MMA, and surfactant, and the reaction time must also be taken into account in these studies in order to obtain the proper conditions for microencapsulation. All things considered, the most plausible explanation for the highly porous microcapsules is the effect of the relatively high concentration of Span 85 (1-6.7% w/v) used to maintain deaggregation of the particles during harvesting. Such concentrations exceed its critical micelle concentration (CMC) and micelles may have interfered with the uniform deposition of polymer.

The outcomes of microencapsulated BHIM with the two polyamides, PLT and PPT, were very different compared to that when PMMA was used. In the first instance, polyamide microcapsules, which were smaller in size (1-4 μm), yielded a much slower release of BHIM at various loadings (22-53%, Table 5.1). Nevertheless, electrocapillary emulsification should have yielded much smaller particles (~200 nm)[65,70]. This may have been due to a slow rate of the polycondensation reaction in the organic phase which resulted in the coalescing of the small particles to form larger particles before the polymerization at the surfaces was complete.

There was a somewhat greater loading of PLT microcapsules with BHIM than with PPT microcapsules although the yields and microencapsulation efficiencies were relatively low. The release kinetics were similar in each case at 23°C and the profiles were characterized by a change in the rate after approximately 20 days to slightly slower values. In the preparation of polyamide microcapsules, protein in the system becomes involved in the interfacial polymerization reaction[69] and, consequently, is bound to the polymer[27]. As a result, the release of protein (BHIM) is considerably slower than if the protein was simply entrapped within the aqueous core of the microcapsules. Furthermore, it follows that low molecular weight protein molecules would diffuse through the polymer matrix faster than large molecular weight molecules. This becomes manifest in the release profiles as time passes and as the microcapsules become depleted of protein. It is not surprising that some differences in the extent to which protein is bound to PLT and PPT microcapsules should occur because of the different structures of the water-soluble monomers used. However, it was not possible to quantitate this. The temperature dependence of protein release from polyamide microcapsules (Fig. 5.6, 5.7) was greatest for PPT microcapsules indicating that the permeability to protein increased to a greater extent than for the PLT microcapsules even though the loading was less for the PPT microcapsules (Table 5.1). Upon examination of the "burst" phases, it can be seen that these were about the same for each of the polyamide microcapsules at the two temperatures. Thus, the faster release of protein from the PPT microcapsules at 40°C is due primarily to protein in the core and not protein bound within the polymer wall. Hence, after 20 days approximately 75 percent of BHIM was lost from PLT microcapsules, compared to 95 percent from PPT microcapsules at 40°C. The rate changes (i.e. slope changes) which occur as a function of time are also more prominent at the higher temperature due to fractionation of the protein sample as it is released through the polymer wall.

In summary, compared to PMMA, both polyamide microcapsules met the objectives of a sustained release for 20-30 days, and a particle size that was in approximately the desired range. However, the process did not permit a sufficiently high yield of robust microcapsules to warrant application in MEOR.

6.2. Dimenhydrinate

It is well known that when microparticles are prepared using a technique such as solvent evaporation used here, the stirring rate of the system influences the product formed[76-77]. In fact, there was a range of stirring rates, and consequently, degree of mixing of the components in the system, over which suitable microspheres could be prepared (300-400 rpm). Indeed, at low stirring rate (200 rpm) microcapsules of dimenhydrinate did not form whereas at high stirring rate (500 rpm) small, irregular-shaped particles resulted. These results emphasize that at least for this system of ethylcellulose and dimenhydrinate there is an optimum stirring rate range, with concomitant solvent evaporation, over which the dynamics of polymer precipitation and simultaneous entrapment of drug particles is appropriate for the formation of microspheres as illustrated in Fig. 5.8. The size distribution of microspheres is unimodal with a lower mean size when prepared at the higher stirring rate (400 rpm) (Fig. 5.9). The coarse sponge-like appearance of the microspheres indicates that the polymer precipitated as strands which coagulated to form the microsphere. Whether the drug became entrapped in the individual strands or within the matrix of the packed strands has not been ascertained but it is likely a combination of both processes, the relative influence of the process being a function of drug loading. Consequently, drug loading at 1:3 polymer:drug ratio was fairly high (~70 %).

In a process of microencapsulation such as this, it is important to validate the effect of preparation conditions on the reproducibility of the microspheres produced in different batches in terms of particle size distribution, the drug loading and within the context of the two acceptable stirring rates employed, and various size fractions isolated by sieving. There was evidence of a significant drug content difference between different sieve size fractions at a 1:3 polymer:drug ratio at 300 rpm but not 400 rpm (Table 5.11). Overall, the results confirm that the microencapsulation technique was reproducible with respect to size distribution and drug content of the microspheres. At ratios representing a lower drug content, it was apparent that the rate of evaporation of solvent (i.e. rate of stirring) was critical for incorporation of drug in polymeric microspheres since at 1:1 polymer:drug ratio at 300 rpm stirring rate, no drug was detected in the microspheres.

The potential of ethylcellulose microspheres of dimenhydrinate as a sustained release drug delivery system is apparent when results of drug release are compared to the dissolution behaviour of drug (Fig. 5.15, 5.16). The higher the drug loading and the smaller the particle size, the greater the release of dimenhydrinate. It is particular noteworthy that even at high drug loadings, such as 1:3 or 1:5 polymer:drug ratios, the release is significantly slower yielding solution drug concentrations (or fraction released) which are considerably less during early released times and extending delivery for 6-8 times longer than that achieved by dissolution (Fig. 5.16). This makes the ethylcellulose microsphere a rather efficient delivery system.

The release kinetics of dimenhydrinate were examined for several of the formulations as a function of the stirring rate, drug loading, and sieve size fractions. Considering the high drug loadings of the formulations, it was not unexpected that the release obeyed first-order kinetics[78] as shown in Fig. 6.1 and Fig. 6.2. However, one formulation, 1:1 polymer:drug microspheres in the 425-841 μm range could be adequately described according to the matrix release model (Higuchi[30]) as can be seen in Fig. 6.3. It can be concluded from this result that the release of dimenhydrinate is probably governed by a dissolution-diffusion mechanism of the drug only. In other words, drug encapsulated in polymer within the microspheres is first released according to matrix diffusion controlled kinetics (Higuchi) into the dispersion medium which permeates the microspheres via the pores and channels extending throughout the microsphere (see Fig. 5.8).

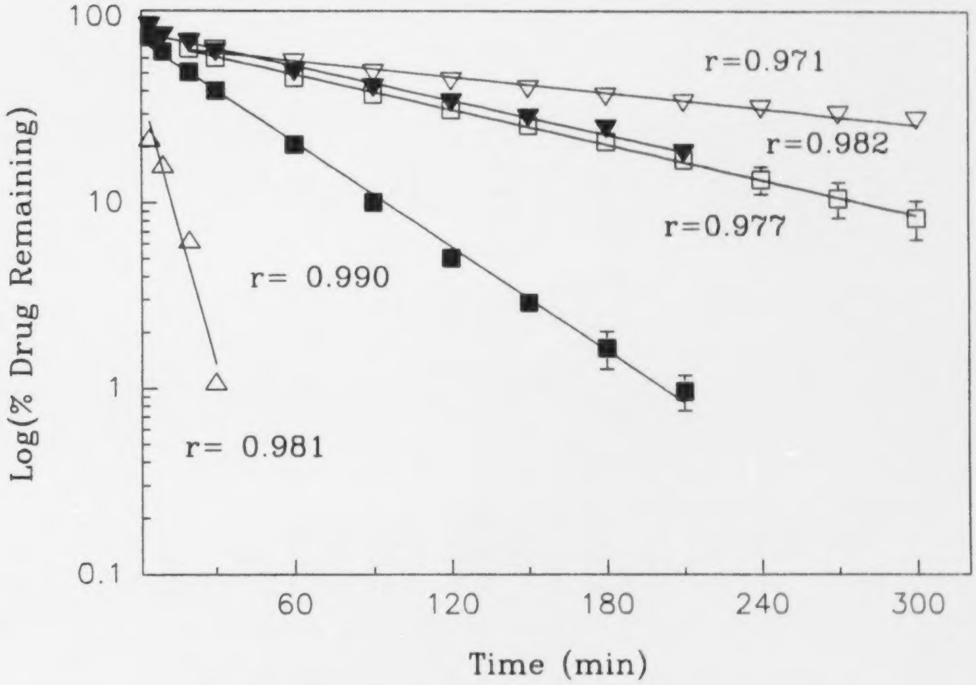

Fig. 6.1. First-order plots of dimenhydrinate remaining versus time for different microspheres prepared at 300 rpm of sieve size ranges, 250-425 μm (closed symbols), 425-841 μm (open symbols). (▾, ▿), 1:3, polymer:drug; (▪, ▫), 1:5, polymer:drug. The dissolution of dimenhydrinate powder (▵), is shown for comparison. Values are the means of measurements from three different batches; bars indicate the standard errors of the means.

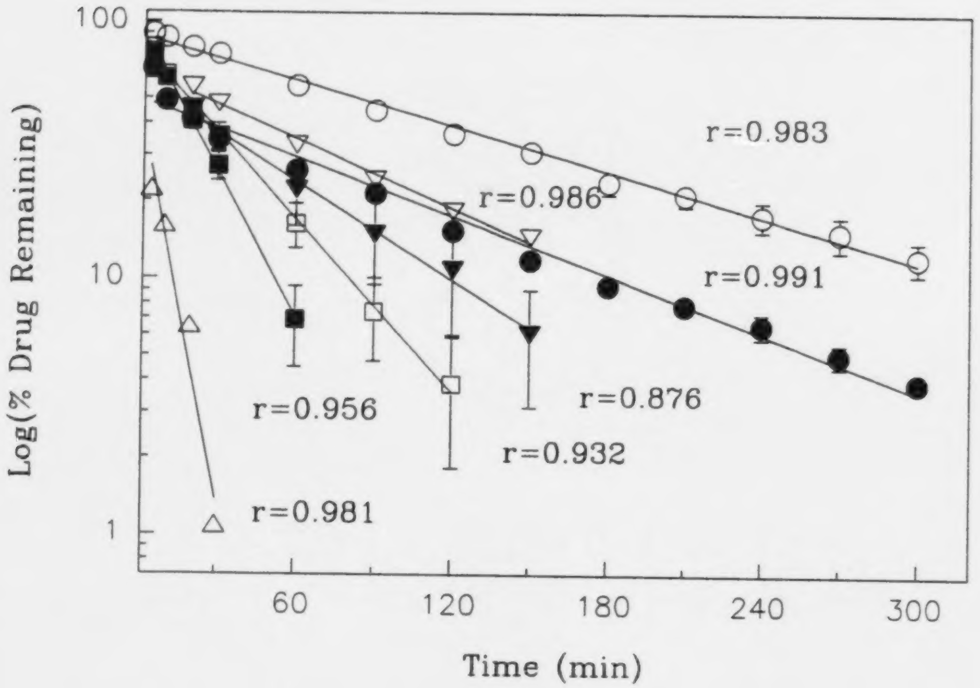

Fig. 6.2. First-order plots of dimenhydrinate remaining versus time for different microspheres prepared at 400 rpm of sieve size ranges, 250-425 µm (closed symbols), 425-841 µm (open symbols). (●, ○), 1:1, polymer:drug; (▼, ▽), 1:3, polymer:drug; (■, □), 1:5, polymer:drug. The dissolution of dimenhydrinate powder (△), is shown for comparison. Values are the means of measurements from three different batches; bars indicate the standard errors of the means.

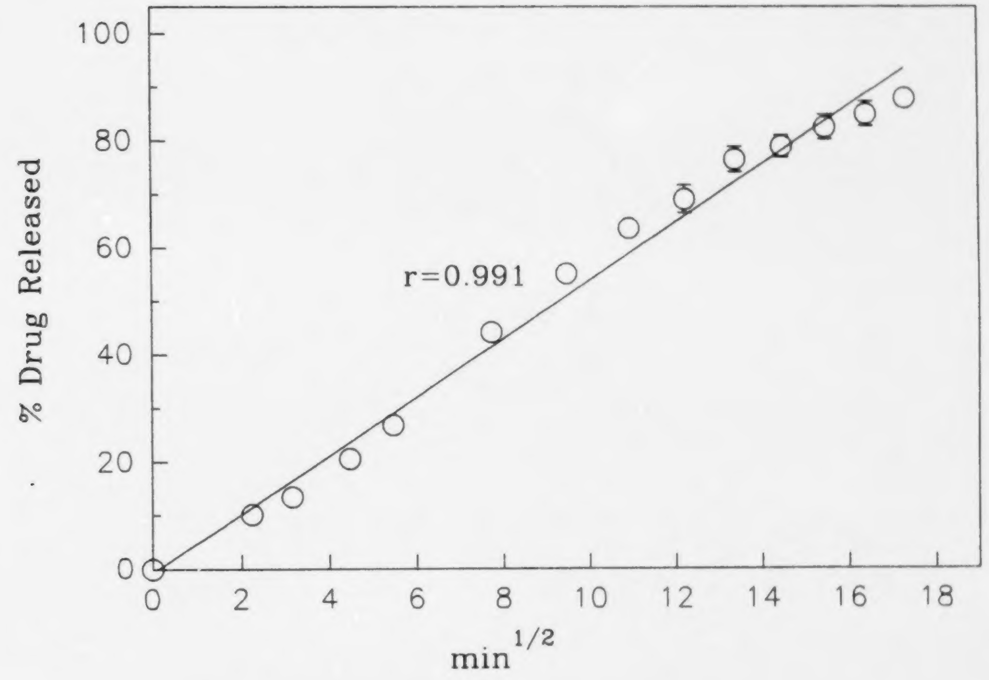

Fig. 6.3. Percentage of dimenhydrinate released versus √time plot for microspheres prepared at 400 rpm of sieve size range 425-841 µm, (○), 1:1, polymer:drug. Values are the means of measurements from three different batches, bars indicate the standard errors of the means.

Table 6.1. First-order release rate constant of dimenhydrinate from ethylcellulose microspheres of sieve size 20/40 and 40/60 prepared under different conditions.

Stirring rates (rpm)	Polymer/Drug	k^a (min^{-1}x10^3)	
		20/40	40/60
300	1/3	3.13±0.29	7.18±1.12
	1/5	7.68±1.08	20.2±1.83
400	1/1	6.18±0.84	8.41±0.60
	1/3	11.4±0.32	18.5±7.74
	1/5	29.1±9.57	46.0±12.7

[a] Values are the average±s.d. of three batches of samples.

Subsequently, drug solution and drug crystals undergoing dissolution that were entrapped within the voids or spaces of the microsphere are delivered to the external medium by first-order kinetics. Thus, the 1:1 polymer:drug formulation in the 425-841 μm sieve size range fits either the first-order or $t^{1/2}$ kinetic model whereas other formulations at higher drug loadings are observed to fit only first-order kinetics, indicating the predominance of the dissolution process compared to the matrix diffusion process at drug loadings greater than 1:1 polymer:drug ratio. The magnitudes of the first-order rate constants (Table 6.1) and the T_{50} values (Table 5.12) are indicative of the effects of particle size, drug loading and the difference in porosities of the microspheres prepared at 300 rpm versus 400 rpm.

6.3. Diphenhydramine HCl

In spite of the reported fragility of Eudragit RS 100 microcapsules observed by Deasy[10] and Kawata[79], it was expected that the hydrophobic nature of this material would significantly slow down the release of a highly water-soluble drug such as diphenhydramine HCl. A similar rationale was used in selecting ethylcellulose N-100. This was not the case. The appearance of the microcapsule in the SEM micrograph (Fig. 5.19) indicates that although the microcapsule surface was not entirely smooth and some drug crystals were observed to be trapped in the polymer, there were no serious defects, pores or otherwise leakage points in the wall. However, a possible reason for the rapid release of drug was revealed during inspection under the optical microscope. Shortly after the sample of microcapsules was dispersed in water for the slide preparation, it was observed that almost all of the microcapsules had burst. An explanation of this behaviour is that water entered the core of the microcapsule under an osmotic pressure gradient causing an internal liquid pressure which, ultimately, fractured the wall causing the microcapsule to disintegrate thereby releasing the drug. Modifying the Eudragit RS 100 and PIB concentrations altered slightly the tendency of this happening, and 8% w/v and 6% w/v, respectively appeared to be the optimum concentrations. PIB is included as an anti-aggregating agent[80] but its presence reportedly affects the wall thickness of the microcapsules produced[81-84].

In conclusion, a suitable material could not be found to prepare stable, sustained release microcapsules of this highly water-soluble drug.

CHAPTER VII

7. CONCLUSIONS

In this research, a high-energy nutrient (BHIM) and an antihistamine have been microencapsulated individually, providing sustained release of these water-soluble agents towards meeting the objectives of the corresponding applications.

In the first investigation, spray drying technique was first selected to prepare microcapsules of BHIM. The particle size of spray dried BHIM powder and PMMA microcapsules of BHIM were reduced to 1-5 μm, however, no sustained release of BHIM was observed because of defects in the microcapsule walls. In-situ polymerization of MMA was then applied to prepare PMMA microcapsules with the expectation that each BHIM solution droplet would assume an uniform polymer coating. However, the walls of these microcapsules possessed many pores. On the other hand, polyamide microcapsules of less than 4 μm in size with BHIM loadings from 20 to 50% were successfully prepared. Sustained release of BHIM for 40 days was also obtained with PLT and PPT microcapsules at 23^{o}C. However, these microcapsules were not robust and had low BHIM encapsulation efficiencies, varying from 3.3 to 8.7%. These represent difficulties in the microcapsules penetrating the mineral formation of a reservoir and supplying sufficient nutrient for growth of UMBs. Consequently, the objective of study of the effect of BHIM microcapsules on the growth rate of UMBs was not tested.

Efforts to formulate sustained release microparticles were successful with one antihistamine, dimenhydrinate, but not the other, diphenhydramine HCl.

1. In general, dimenhydrinate microspheres prepared were spherical and had particle sizes ranging from 125 to 841 μm.
2. Dimenhydrinate microspheres prepared under different conditions were reproducible with respect to particle distribution and drug content.
3. Drug loadings varied from 40 to 115 percent of the theoretical values, depending upon the initial amount of dimenhydrinate during preparation. Overall, the higher the drug to polymer ratio, the higher was the drug loading.
4. Depending on the particle size and drug loading, dimenhydrinate release from ethylcellulose microspheres ranged from 1 to 10 hr.
5. The first-order kinetic profiles of dimenhydrinate release from ethylcellulose microspheres could be explained by a dissolution-diffusion mechanism.
6. The high water solubility of diphenhydramine HCl was responsible for a rapid increase in pressure within the microcapsule due to the osmotic pressure gradient causing fracturing and disintegration of some microcapsules and rapid release of the drug to the external medium.

REFERENCES

1. H. G. Bungenburg de Jong and A. J. Kass, Zur Kenntuis der Komplex-koazeration, V. Mitteilung : relative verschiebunger, im elektrischen gleichstromfelde von flussigkeits-einschliebungen inn komplex-koazervat-trofehen, *Biochem.* Z. 232: 338-345, (1931) (taken from ref. 10).
2. B. K. Green and L. Scheicheer, U. S. Patent 2,730,456 (1956) (taken from ref. 10).
3. B. K. Green and L. Scheicheer, U. S. Patent 2,730,457 (1956) (taken from ref. 10).
4. B. K. Green and L. Scheicheer, U. S. Patent 2,800,457 (1957) (taken from ref. 10).
5. R. E. Sparks, Comparison of microencapsulation processes for controlled release of drugs and chemicals, *Polym. Sci. Technol.* 34: 421-27, (1986).
6. A. Kondo, *Microcapsule Processing and Technology*, J. Wade Van Valkenburg, ed., Dekker, New York, (1979).
7. R. E. Sparks, Microencapsulation in *Kirk-Othmer Encyclopedia of Chemical Technology*, Vol. 15, 3rd., John Wiley and Sons, p. 470-493, (1981).
8. M. H. Gutcho, *Microcapsules and other capsules*, Noyes Data Corporation, New Jersey, (1979).
9. J. R. Nixon ed., *Microencapsulation*, Dekker, New York, (1976).
10. P. B. Deasy, *Microencapsulation and related drug processes*, Mercel Dekker, New York, (1984).
11. A. F. Kydonieus, *Controlled release technologies: Method, Theory, and Applications*, CRC Press, Florida, (1980).
12. R. Arshady, Naming microcapsules, *J. Microencapsulation*, 9(2): 187-90, (1992).

13. W. Sliwka, Microencapsulation, *Angew. Chem. Internat. Edit.* 14(8): 539-50, (1975).

14. C. Thies, Microencapsulation as drug delivery devices, *CRC Crit. Rev. Biomed. Eng.* 8(4): 335-381, (1982).

15. R. Arshady, *Polym. Eng. Sci.*, 29(24): 1746-58, (1989).

16. J. L. Gardon, *High Polymers*, 29: 143, (1977).

17. K. E. J. Barret, *Dispersion Polymerization in Organic Media*, John Wiley, London, (1975).

18. T. M. S. Chang, *Artificial Cells*, Thomas, Springfield, III, (1972).

19. P. B. Deasy, Microencapsulation of drugs by pan and air suspension techniques, *Crit. Rev. Ther. Drug Carrier Syst.*, 8(1): 39-89, (1991).

20. K. Master, *Spray drying handbook*, 3rd ed., George Godwin, London, (1979).

21. D. E. Wurster, U. S. Patent 2,648,609, (1953); 2,799,241, (1957) (taken from ref. 11).

22. T. R. Tice and R. M. Gilley, Preparation of injectable controlled-release microcapsules by a solvent-evaporation process, *J. Controlled Release,* 2: 343-352, (1985).

23. R. Ashady, Microspheres and microcapsules : A survey of manufacturing techniques. Part 1. Suspension crosslinking, *Polym. Eng. Sci.*, 29(24): 1746-1758, (1989).

24. R. W. Croswell and C. H. Becker, Suspension polymerization for preparation of timed-release dosage forms, *J. Pharm. Sci.*, 63(3): 440-442, (1974).

25. B. Ekman and I. Sjoholm, Improved stability of proteins immobilized in microparticles prepared by a modified emulsion polymerization technique, *J. Pharm. Sci.*, 67(5): 693-696, (1978).

26. Pateco, U. S. Patent 3,330,693 (1967) (taken from ref. 6).

27. T. M. S. Chang, Semipermeable microcapsules, *Science*, 146: 524-525, (1964).

28. R. W. Baker and H. K. Lonsdale, Controlled release: mechanisms and rates, in *Experimental Biology and Medicine*, A. C. Tranquary and R. E. Lacey, eds., Plenum Press, New York, p. 15-64, (1974).

29. T. Higuchi, Rate of release of medicaments from ointment bases containing drugs in suspension, *J. Pharm. Sci.*, 50(12): 874, (1961).

30. T. Higuchi, Mechanism of sustained-action medication, *J. Pharm. Sci.*, 52: 1145, (1963).

31. S. J. Desai, P. Singh, A. P. Simonelli, and W. I. Higuchi, Investigation of factors influencing release of solid drug dispersed in inert matrics II: Quantitation of procedures, *J. Pharm. Sci.*, 55: 1224, (1965).

32. S. J. Desai, P. Singh, A. P. Simonelli, and W. I. Higuchi, Investigation of factors influencing release of solid drug dispersed in inert matrices III. Quantitative studies involving the polyethylene plastic matrix, *J. Pharm. Sci.*, 55: 1230, (1966).

33. S. J. Desai, P. Singh, A. P. Simonelli, and W. I. Higuchi, Investigation of factors influencing release of solid drug dispersed in inert matrices IV. Some studies involving the polyvinyl chloride matrix, *J. Pharm. Sci.*, 55: 1235, (1966).

34. R. Langer, Polymeric delivery systems for controlled drug release, *Chem. Eng. Commun.*, 6: 1-48, (1980).

35. H. B. Hopfenberg, *Controlled release from erodible slabs, cylinders, and spheres, in controlled release polymeric formulation*, D. R. Paul and F. W. Harris, ed., American Chemical Society, Washington, p. 26, (1976).

36. J. Heller and R. W. Baker. *Theory and practice of controlled drug delivery from bioerodible polymers*, in 6th International symposium on controlled

release of bioactive materials, R. W. Baker, ed., Academic Press, New York, Chapter I, (1980).

37. L. G. Donaruma, Synthetic biologically active polymers, *Progress in Polymer Sci.,* 4, A. D. Jenkins, ed., Pergamon Press, Oxford (1975).
38. H. Ringsdorf, Synthetic polymeric drugs in *Polymer Delivery Systems,* Midland Macromolecular Symposium 5, R. J. Kostelnik, ed., Gordon and Breach, New York, p. 197. (1978).
39. A. Trouet, Carrier for bioactive materials in *Polymeric Delivery Systems*, Midland Macromolecular Symposium 5, R. J. Kostelnik, ed., Gordon and Breach, New York, p. 157. (1978).
40. E. Goldberg. Polymeric affinity drugs, in *Polymeric Delivery Systems*, Midland Macromolecular Symposium 5, R. J. Kostelnik, ed., Gordon and Breach, New York, p. 227. (1978).
41. H. B. Hopfenberg and K. C. Hsu, Swelling-controlled constant rate delivery system, *Polym. Eng. Sci.*, 18: 1186, (1978).
42. W. G. Chambliss, R. W. Cleary, R. Fisher, A. B. Jones, P. Skierrkowski, W. Nicholes, and A. H. Kibbe, Effect of docusate sodium on drug release from a controlled-release dosage form, *J. Pharm. Sci.*, 70: 1248-51, (1981).
43. T. J. Roseman and W. I. Higuchi, Release of medroxyprogesterone acetate from a silicone polymers, *J. Pharm. Sci.*, 59: 353, (1972).
44. Y. Samuelov, M. Donbrow, and M. Friedman, Sustained release of drugs from ethylcellulose-polyethylene glycol films and kinetics of drug release, *J. Pharm. Sci.*, 68: 325, (1979).
45. I. Jalsenjak, C. F. Nicolaidou, and J. R. Nixon, The *in vitro* dissolution of phenobarbitone sodium from ethyl cellulose microcapsules, *J. Pharm. Pharmacol.*, 28: 912, (1976).
46. P. L. Madan, Clofibrate microcapsules: III Mechanism of release, *Drug, Dev.*

Ind. Pharm. 6: 629-44, (1980).

47. W. M. Edwards, L. L. Harrold, Agricultural pollution of water bodies, *Ohio J. Sci.*, 70(1): 50-56, (1970).

48. D. H. Lewis and D. R. Cowsar, *Principles of controlled release pesticides, in Controlled Release Pesticides*, H. B. Schere ed., ACS symposium series 53, (1977).

49. Y. T. Gao and B. H. Wang, Safety comparison of insecticide microencapsulation and investigation of its mechanism, *J. Microencapsulation*, 6(4): 527-33, (1989).

50. R. C. Koestler, In *Proceeding 1976 Controlled release pesticide symposium*, N. F. Cardarelli, ed., Unversity of Akron, Ohio, (1974).

51. E. E. Ivy, Penncap-M®: an improved methyl parathion formulation, *J. Econ. Entomol.*, 65: 473, (1972).

52. H. Hall and T. Hinkes, Wurster process for controlling pesticides, in *Pro. 1976 Int. Controlled release pesticide symposium.*, Cardarelli, N. F. ed., Unversity of Akron, Ohio, 4.1, (1976).

53. J. Abrams and T. Hinkes, Encapsulation of solid particles, in *Proc. 1974 Int. Controlled release pesticide symp.*, Cardarelli, N. F. ed., Unversity of Akron, Ohio, 7.1, (1974).

54. J. Leonard, Annual production report. Increase rate of EOR brightens outlook. *Oil & Gas J.* April, p. 71-101, (1986).

55. F. Cusack, H. M. Lappin-Scott and J. W. Costeron, Bacteria can plug waterflood injection wells, *Oil & Gas J.* Nov., 9: 59-64, (1987).

56. J. C. Shaw, B. Bramhill, N. C. Wardlaw, and J. W. Costerton, Bacteria fouling in a model core system, *Appl. Environ. Microbiol.* 49: 693-701, (1985).

57. F. A. MacLeod, H. M. Lappin-Scott, and J. W. Costerton, Plugging of a model rock system by using starved bacteria, *Appl. Environ. Microbiol.* 54(6): 1365-72, (1988).

58. H. M. Lappin-Scott, F. Cusack, and J. W. Costerton, Nutrient resuscitation and growth of starved cells in sandstone cores: a novel approach to enhanced oil recovery, *Appl. Environ. Microbiol.* 54(6): 1373-82, (1988).

59. V. L. McKincey, J. W. Costerton, and D. C. White, Microbial biomass, activity, and community structure of water and particulates retrieved by backflow from a waterflood injection well, *Appl. Environ. Microbiol*, 54(6): 1383-93, (1988).

60. V. L. Newlove and L. A. McDougall, U. S. Patent 4,660,645, (1987).

61. L. A. McDougall, J. C. Newlove, J. A. Haslegrave, U. S. Patent 4,670,166, (1987).

62. C. R. Charck, D. L. Whitfill, D. P. Corda, E. F. McBride and H. E. Bellis, U. S. Patent 4,986,353, (1991).

63. L. A. Cantu and M. E. Yost, U. S. Patent 4,986,354, (1991).

64. R. Bodmeier and H. G. Chang, Preparation of biodegradable poly(±) lactide microparticles using a spray-drying technique, *J. Pharm. Pharmacol.*, 40: 754-757, (1988).

65. M. Arakawa and T. Kondo, Preparation and properties of poly(N^{α}, N^{ζ}, L-lysinediyterephthaloyl) microcapsules containing hemolysate in the nanometer range, *Can. J. Physiol. Pharmacol.*, 58: 183-187, (1980).

66. *American Hospital Formulation Services*, 4:00 Antihistamine drugs p. 16-17.

67. J. M. Scavone, B. G. Luna, J. S. Harmatz, Diphenhydramine kinetics following intravenous, oral, and sublingual dimenhydrinate adminstration, *Biopharm. Drug Dispos.* 11(3): 185-9, (1990).

68. O. Lowry, N. Rosenbergh, A. Farr and R. Randall, *J. Biol. Chem.*, 193: 256,

(1951).

69. P. L. Morgan and S. L. Kwolek, Interfacial polycondensation. II. Fundamentals of polymer formation at liquid interfaces, *J. Polymer Sci.*, 40: 289, (1959).

70. A. Watanabe, K. Higashitsuji and K. Nishizawa. Studies on electrocapillary emulsification, *J. Colloid Interface Sci.*, 64(2): 278-89, (1978).

71. M. Arakawa and T. Kondo, Preparation of hemolysate-loaded poly (N^{α}, N^{ζ}, L-lysinediylterephthaloyl) nanocapsules, *J. Pharm. Sci.*, 70(4): 354-357, (1981).

72. H. P. Huang and I. Ghebre-Sellassie, Preparation of microspheres of water-soluble pharmaceuticals, *J. Microencapsulation*, 6(2): 219-25, (1987).

73. A. C. Shah, C. B. Peot and J. F. Ochs, Design and evaluation of a rotating filter-stationary basket *in vitro* dissolution test apparatus I: fixed fluid volume system, *J. Pharm. Sci.*, 62(4): 671-677, (1973).

74. S. Benita and M. Donbrow, Effect of polyisobutylene on ethylcellulose-walled microcapsules: wall structure and thickness of salicylamide and theophylline microcapsules, *J. Pharm. Sci.*, 71: 205, (1982).

75. S. Benita, A. Hoffman and M. Donbrow, Microencapsulation of paracetamol using polyacrylate resins (Eudragit Retard), kinetics of drug release and evaluation of kinetic model., *J. Pharm. Pharmacol.*, 37: 391-5, (1985).

76. R. Bodmeier, H. Chen, P. Tyle and P. Jarosz, Pseudoephedrine HCL microspheres formulated into an oral suspension dosage form, *J. Controlled Release*, 15: 65-77, (1991).

77. R. Alex and R. Bodmeier, Encapsulation of water-soluble drugs by a modified solvent evaporation method. I. Effect of process and formulation variables on drug entrapemnt, *J. Microencapsulation*, 7(3): 347-355, (1990).

78. S. Benoît, S. Benita, F. Puisieux and C. Thies, Stability and release kinetics

of drugs incorporated within microspheres, in *Microspheres and drug therapy*, S. S. Davis et al., edited. Elsevier, Amsterdam. New York. Oxford, (1984).

79. M. Kawata, M. Nakamura, S. Goto and T. Aoyama, Preparation and dissolution of Eudragit RS microcapsules containing ketoprofen, *Chem. Pharm. Bull.* 34(6): 2618-2623, (1986).

80. M. Donbrow, A. Hoffman and S. Benita, Phase separation modulation and aggregation prevention: mechanism of the non-solvent addition method in the presence and absence of polyisobutylene, *J. Microencapsulation,* 7(1): 1-15, (1990).

81. S. Benita and M. Donbrow, Effect of polyisobutylene on ethylcellulose-walled microcapsules: wall structure and thickness of salicylamide and theophilline microcapsules. *J. Pharm. Sci.* 71(2): 205-210, (1982).

82. Y. Kawashima, S. Y. Lin, A. Kasai, H. Takenaka, K. Matsunami, Y. Nochida and H. Hirose, Drug release properties of the microcapsules of adriamycin hydrochloride with ethylcellulose prepared by a phase separation techniques, *Drug Development and Industrial Pharmacy*, 10(3): 467-479, (1984).

83. J. R. Nixon, G. A. Agyilirah, The effect of polyisobutylene on the properties of ethylcellulose-walled microcapsules of phenobarbitone sodium, *Acta Pharmaceutica Technologica*, 28(2): 137-140, (1982).

84. M. Samejima, G. Hirata and Y. Koida, Studies on microcapsules I. Role and effect of coacervation-inducing agents in the microencapsulation of ascorbic acid by a phase separation method, *Chem. Pharm. Bull.* 30(8): 2894-2899, (1982).

APPENDIX

Spectrophotometric Analysis of BHIM

A calibration curve of absorbance values of BHIM solution vs. their BHIM concentrations over the range of 5 to 400 μg/ml was obtained by using the Lowry protein assay. Second order regression analysis of the experimental values yielded a relationship between absorbance and concentration of $A = 2.9\text{x}10^{-2} + 2.9\text{x}10^{-3}C - 2.76\text{x}10^{-6}C^2$, with a correlation coefficient, $r = 0.9977$. Reproducibility of the experimental values was always > 99.2%.

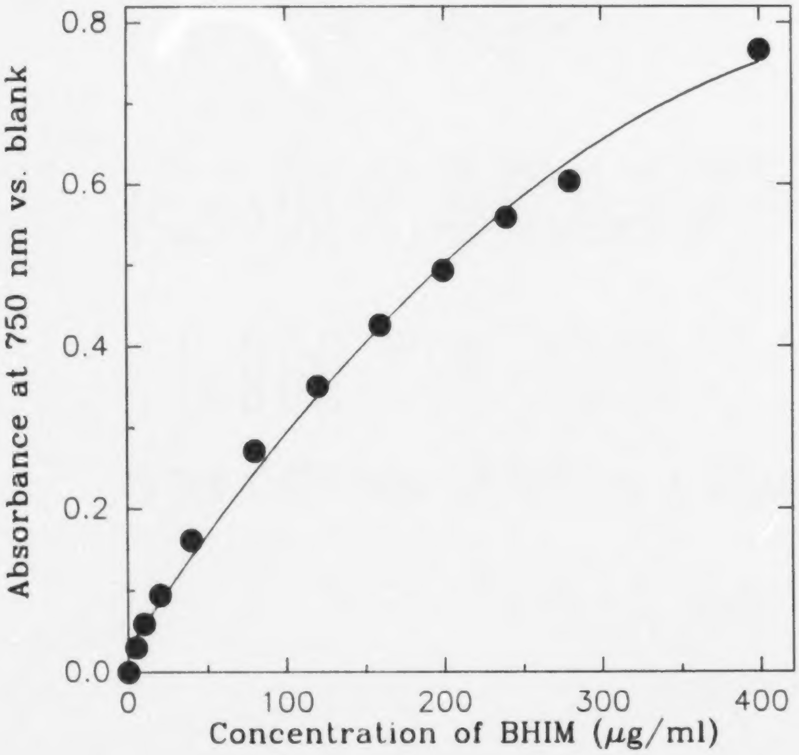

UV Spectrophotometric Analysis of Dimenhydrinate

A linear calibration curve which obeyed Beer's law over the concentration range of 1.5 to 30 μg/ml in water was obtained for concentration determination in release studies. Regression analysis of the experimental values yielded a slope = 0.028, intercept = 0.000, and correlation coefficient, r = 0.9999. Reproducibility of the experimental values was always > 99%.

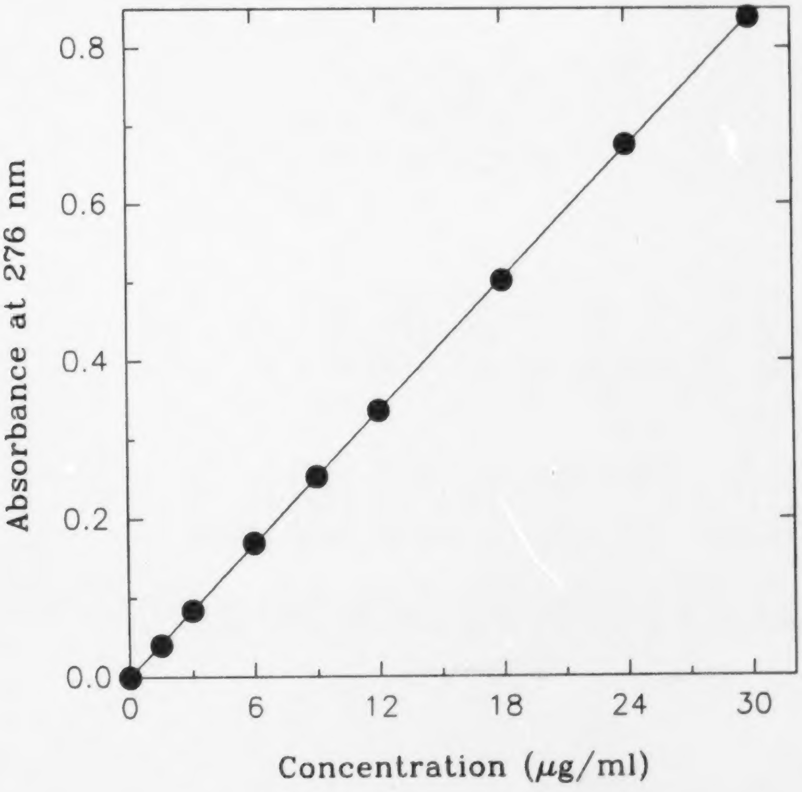

UV Spectrophotometric Analysis of Dimenhydrinate

A linear calibration curve which obeyed Beer's law over the dimenhydrinate concentration range of 1.5 to 30 μg/ml in 95% ethanol was obtained for encapsulation efficiency determination. Regression analysis of the experimental values yielded a slope = 0.027, intercept = 0.008, and a correlation coefficient, r = 0.9998. Reproducibility of the experimental values was always > 99%.

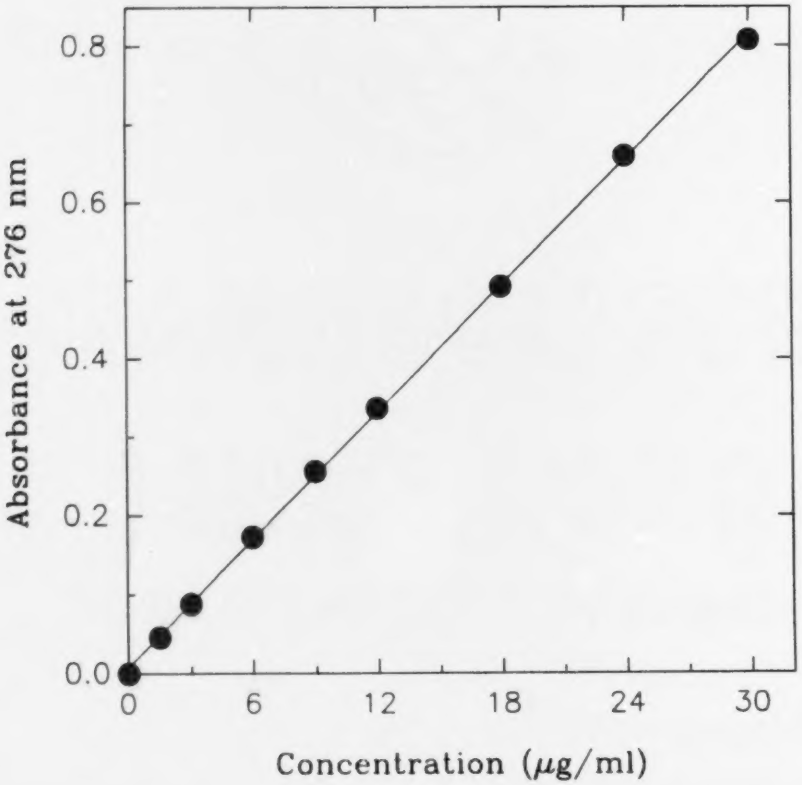

UV Spectrophotometric Analysis of Diphenhydramine HCl

A linear calibration curve which obeyed Beer's law over the concentration range of 20 to 400 μg/ml in pH 7.4 phosphate buffer was obtained for concentration determination in release studies. Regression analysis of the experimental values yielded a slope = 0.0016, intercept = -4.44×10^{-4}, and correlation coefficient, r = 0.9993. Reproducibility of the experimental values was always > 99%.

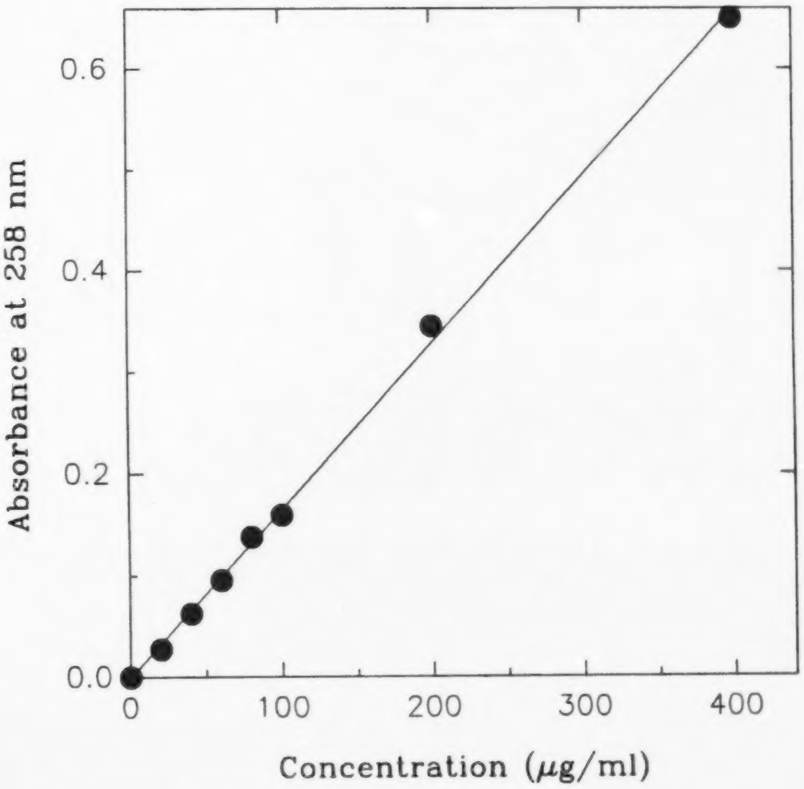

UV Spectrophotometric Analysis of Diphenhydramine HCL

A linear calibration curve which obeyed Beer's law over the diphenhydramine HCl concentration range of 20 to 400 µg/ml in 95% ethanol was obtained for encapsulation efficiency determination. Regression analysis of the experimental values yielded a slope = 0.0011, intercept = 0.0031, and correlation coefficient r = 0.9999. Reproducibility of the experimental values was always > 99%.